Petroleum Science 19 (2022) 2343–2357

Contents lists available at ScienceDirect

Petroleum Science

journal homepage: www.keaipublishing.com/en/journals/petroleum-science

Review

Crude oil wax: A review on formation, experimentation, prediction, and remediation techniques

Wyclif Kiyingi [a], Ji-Xiang Guo [a, *], Rui-Ying Xiong [a], Li Su [b], Xiao-Hui Yang [b], Shi-Ling Zhang [c]

[a] Unconventional Petroleum Research Institute, China University of Petroleum, Beijing, 102249, China
[b] Sinopec Northwest Oil Field Branch, Urumqi, Xinjiang, 830011, China
[c] CNPC Engineering Technology R&D Company Limited, Beijing, China

ARTICLE INFO

Article history:
Received 8 September 2021
Received in revised form
1 August 2022
Accepted 11 August 2022
Available online 20 August 2022

Edited by Xiu-Qiu Peng

Keywords:
Oil wax
Phase modeling
Inhibitors
Dispersants
Multi-phase flow

ABSTRACT

Wax deposition during crude oil production, transportation, and processing has been a headache since the early days of oil utilization. It may lead to low mobility ratios, blockage of production tubing/pipelines as well as fouling of surface and processing facilities, among others. These snags cause massive financial constraints increasing projects' turnover. Decades of meticulous research have been dedicated to this problem that is worth a review. Thus, this paper reviews the mechanisms, experimentation, thermodynamic and kinetic modeling, prediction, and remediation techniques of wax deposition. An overall assessment suggests that available models are more accurate for single than multi-phase flows while the kind of remediation and deployment depend on the environment and severity level. In severe cases, both chemical and mechanical are synergistically deployed. Moreover, future prospective research areas that require attention are proposed. Generally, this review could be a valuable tool for novice researchers as well as a foundation for further research on this topic.

1. Introduction

Crude oil is a complex multi-component organic mixture consisting mainly of hydrocarbons and a few non-hydrocarbons. The general composition is categorized into saturates, aromatics, resins, and asphaltenes (Xiong et al., 2020a, 2020b). Some of the saturate compounds have high melting points, hence easily solidifying at low temperatures. They precipitate out of the fluid as the temperature drops to a certain degree - typically below 80 °C - to form colloids known as wax. The wax forming molecules are mainly normal and branched alkanes though some naphthenes attached to long carbon chains are also possible wax forming molecules. The deposition of wax in the oil and gas industry is both an economic and operational challenge. These problems occur during production, transportation, and storage. Amongst them are blockage of well tubing and transport pipelines (Fig. 1); reduction of the drawdown pressure; fouling of surface facilities like separators and tankers; and increased energy input for pumps.

As energy consumption across the globe continues to increase at an exponential rate, so are the conventional reserves being exponentially depleted. This phenomenon has propelled the quest to explore alternative energy sources and led to increased production from offshore oil reserves in addition to other extreme climatic environments over the past decade (Bai and Bai, 2018). Production from these fields sometimes requires transportation of crude oil over long distances to processing facilities. If proper counter control measures are not implemented, oil temperature may drop to that of the environment, causing precipitation of wax from the oil. When this deposition is significantly high, it can cause operational problems that may dump cold water on the economic prospects of projects due to the costly remedies required.

In most cases, this problem is inevitable as numerous waxy oil fields are spread across the globe, yet no single universal solution exists (Batsberg et al., 1991; Del Carmen Garcia, 2001; Ding et al., 2006; Rønningsen, 2012; Pedersen et al., 1991; Suppiah et al., 2010). Most companies adapt pigging as the most preferred remediation technology. However, it should be noted that this technology is also associated with some shortcomings like an

* Corresponding author.
E-mail address: guojx002@163.com (J.-X. Guo).

https://doi.org/10.1016/j.petsci.2022.08.008

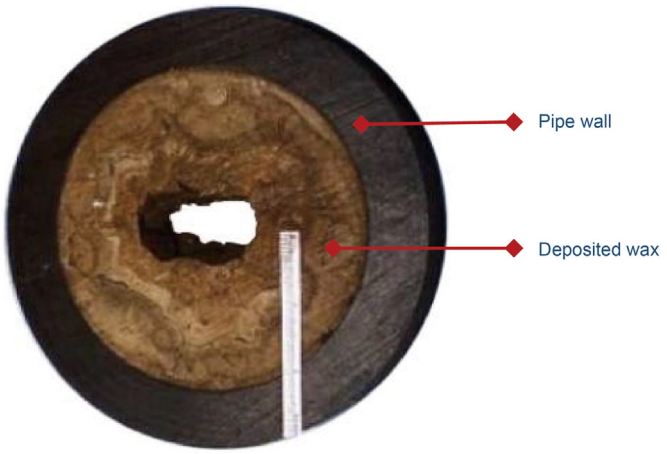

Fig. 1. Cross-section cut through a pipe plugged with wax. Adapted with permission from Singh et al. (2000). Copyright © 2000 American Institute of Chemical Engineers (AIChE).

interruption of production operations. Moreover, its frequency also adds extra costs (like single pigging power, electric and thermal costs) to the overall production budget (Niesen, 2002; Xie et al., 2018).

1.1. Structure

As earlier mentioned, wax is mainly composed of normal and slightly branched alkanes but also can include naphthenes with long alkane chains that precipitate during the wax formation process (Fig. 2).

1.2. Chemical composition

According to Bishop et al.'s experimental investigation of high molecular weight hydrocarbons, it was revealed that wax forming alkanes were mainly light compounds with relatively low carbon numbers (C_{20}–C_{50}). In contrast, those heavier than C_{50} are scarce in solid wax (Philp et al., 1995). This was attributed to the concentration pattern of alkanes/paraffins, that is to say, normal alkanes and slightly branched iso-paraffins that exist in considerable amounts within the lighter C_{7+} fractions. The degree of branching in heavier fractions is more pronounced; thus, molecules are less likely to enter into a solid structure. Alkane components with little or no branching are found in high concentrations within the lighter C_{7+} fractions, but due to their low melting points, the amount in solid wax is limited by the temperature constraint. Therefore, the solid wax phase predominantly comprises C_{20}–C_{50} alkanes.

2. Wax deposition

2.1. Wax formation

As oil temperatures drop to a certain degree, the wax may start to deposit as a solid layer inside the pipeline. If not mitigated, the layer builds up with continued transport and eventually plugs the pipeline. Albeit not all formed wax deposits on the wall, some crystals remain suspended as solid particles in the liquid phase (Fig. 3). This process is mainly dependent on temperature and composition factors. When the crude oil temperature drops to the wax appearance temperature (WAT), paraffin molecules in the oil start to precipitate out of the fluid liquid phase forming minute crystalline solids. If conditions prevail, further temperature drops cause the solids to aggregate, thus creating a gel-like matrix composed of trapped oil and wax particles that later deposits on the walls of the pipe, Fig. 3(b).

Although studies have shown that wax deposition is mainly dependent on temperature and oil composition, this has not restricted research on other factors like flow regimes and flow velocities (Quan et al., 2020; Taheri-Shakib et al., 2020; Zhou et al., 2020).

2.2. Precipitation mechanism

Initially, Brownian motion, molecular diffusion, shear dispersion, and gravity were attributed to be the causative mechanisms behind the wax formation, but as years have gone by, some of these mechanisms have been refuted. Moreover, new ones like nucleation, shear stripping, and aging have been added to the list (Haj-Shafiei et al., 2019; Hoffmann et al., 2012).

2.2.1. Brownian motion, shear dispersion, and gravity

Some research works have cast shadows on the validity of these mechanisms for various reasons. Brownian motion - haphazard motion of tiny particles-was proposed to deposit wax molecules at the center of the pipes (Burger et al., 1981). It has been argued that because of the low temperature at the walls of the line compared to the system temperature, it's not realistic to suggest that the mechanism is the cause for deposition on the walls (Singh et al., 2000).

Moreover, gravity effects attributed to differences in oil and wax particle densities result in the settlement of wax particles due to gravitation force. This mechanism may be viable in horizontal

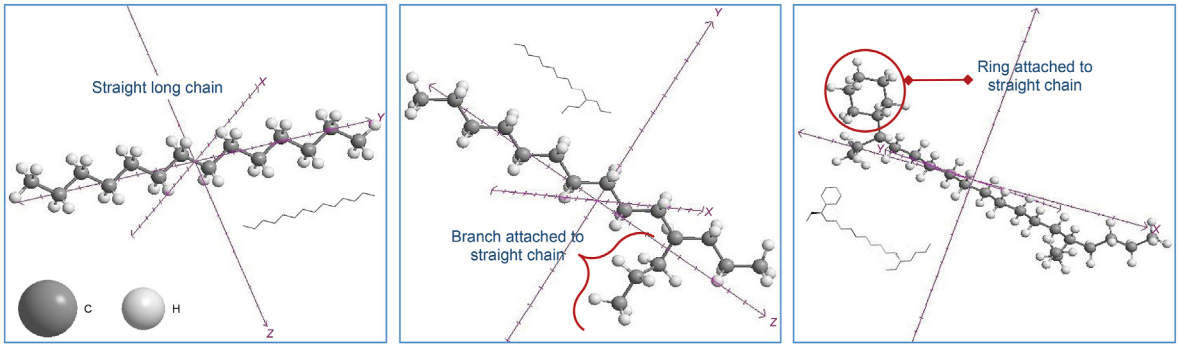

Fig. 2. Waxy forming alkane species.

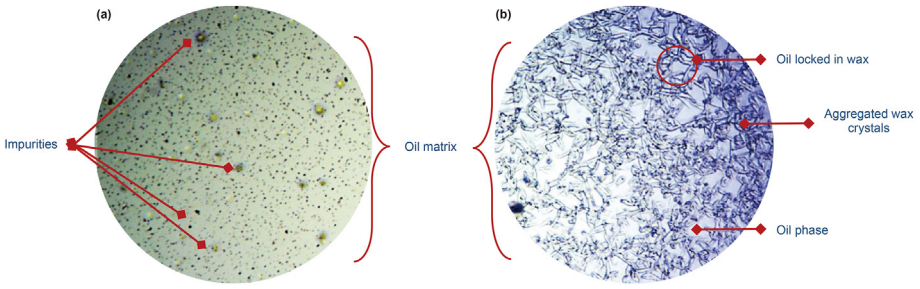

Fig. 3. Microscopic view of wax crystallization in oil using commercial wax (high power magnification ×40) (**a**) Blank oil sample; (**b**) Oil mixed with 2 wt% commercial wax.

pipelines, but the concept is less probable in vertical tubes/pipes (Burger et al., 1981; Mansourpoor et al., 2019a,b).

Shear dispersion is due to the existence of velocity gradients during oil flow (Hsu et al., 1994). It is conferred that because the particles' velocity decreases towards the wall while at maximum velocity towards the center of the flow, a velocity gradient exists that leads to wax deposition onto the pipe walls. However, while this mechanism seems convincing when considering laminar flows, it fails to account for deposition in more dynamic conditions such as turbulent flow, which tend to remove particles from the stationary state to the bulk fluid (Bird, 2002; Lee et al., 2020; Saffman, 1965). The mechanism has been generally neglected in several depositional models (Hernandez et al., 2003; Huang et al., 2011a,b; Semenov, 2012; Singh et al., 2000).

2.2.2. Molecular diffusion

Molecular diffusion, illustrated in Fig. 4, explains the deposition of wax molecules from high concentration regions (center of the tube) to low concentration regions due to a temperature gradient that exists as the oil temperature drops to and below the wax appearance temperature (Burger et al., 1981; Hoffmann et al., 2012; Matzain, 1996; Singh et al., 2000). Presently, this mechanism has gained consensus among the scientific community as the primary drive mechanism behind wax deposition (Alnaimat and Ziauddin, 2020; Huang et al., 2011a,b; Wang et al., 2013, 2018; P. Wang et al., 2013). Generally, Fick's law of diffusion has been used to incorporate this mechanism into depositional models.

2.2.3. Nucleation/emulsified nucleation

This mechanism has attracted attention given that during oil production. Emulsions are formed due to a multitude of reasons, such as pump actions, among others. Under low-temperature conditions, emulsified particles coalesce, forming a deposition surface for wax molecules. The wax formation is initiated by the formation of very minute solid particles and is followed by the continuous growth of particles as molecules are progressively added. In the course of this process, the minute crystals are adsorbed onto the dispersed phase, followed by agglomeration that forms a network of wax crystals as temperature continuously drops below the WAT. This structural network locks oil in its matrix, rendering it immovable, forming a gel (gelation) (Hoffmann et al., 2012). Consequently, this gel-like solid deposits onto the walls.

2.2.4. Aging

Wax molecules on the wax deposit's surface infuse into the deeper sections of the deposit, reinforcing its mechanical properties like thickness and hardness (Hernandez et al., 2003; Huang et al., 2011a,b; Matzain, 1996). The mechanism is dependent on temperature dissipations and varies in different crude compositions. It is valid to suggest that shear stripping and this mechanism supplement each other. The effused oil molecules are stripped away while the wax fills the space left behind.

2.2.5. Shear stripping

As discussed earlier, some oil is locked in the pores of the matrix; this mechanism mainly contributes to hardening the deposit by stripping away the oil molecules with flow energy while the wax

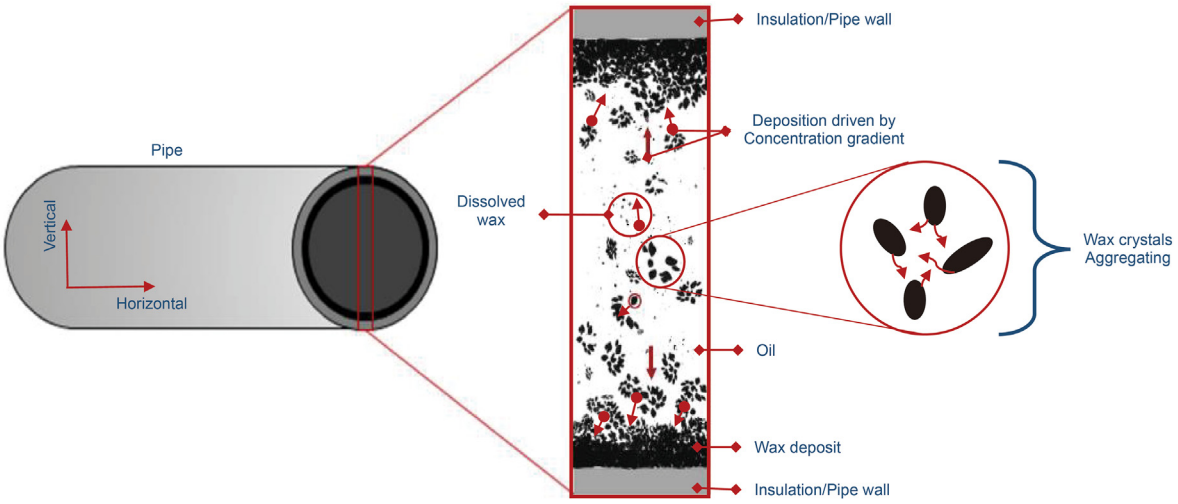

Fig. 4. Illustration of wax molecular diffusion theory for its deposition.

molecules migrate to fill the spaces in the matrix (Quan et al., 2019).

Research on these mechanisms has significantly contributed to the advancements in predictive models, as discussed in the following sections.

3. Wax prediction

Prediction of wax deposition requires both thermodynamic and deposition modeling. In this section, a review of progress on these topics is provided.

3.1. Thermodynamic modeling

Wax formation is an exothermic process involving creating a solid ordinate structure from a thermodynamically unstable phase system. Lashkarbolooki et al. noted that the presence of an excess chemical potential for a solute in comparison to its equilibrium might lead to the formation of wax crystals (Lashkarbolooki et al., 2010, 2011).

Thermodynamic modeling predicts the onset of wax deposition and amount at various temperature–pressure conditions through phase equilibria when the oil is accurately characterized. Predictive models have been postulated by tracking changes in the distribution of crude components with respect to temperature and pressure (Bagherinia et al., 2016, 2019; Benamara et al., 2019).

Thermodynamically, wax crystals exist in a three-phase equilibrium system at an equilibrium state, as illustrated in Fig. 5. This state qualifies this kind of system as a multi-component system. Therefore, equilibrium calculations for such systems require a thorough comprehension of the states' fugacities (fugacity coefficients) for each component in the system (Chueh and Prausnitz, 1967; Pedersen et al., 1984, 1991; Won, 1986). These are essential because they are measurable quantities that are related to the Gibbs free energy of the individual components (Elliott and Lira, 1999; Smith et al., 1996). At equilibrium, the fugacities of individual components should be equal, as shown in Fig. 5 and given by Eq. (1).

$$f_i^{\mathrm{v}} = f_i^{\mathrm{l}} = f_i^{\mathrm{s}} \tag{1}$$

where $f_i^{\mathrm{v}}, f_i^{\mathrm{l}}$ and f_i^{s} are the fugacities for the vapor, liquid, and solid-phase components.

Over the past decades, several scholars have attempted to model the precipitation of wax in crude oils based on its thermodynamic state. Among the most recognized in the industry are: Won's method (1986, 1989), Pedersen (1995), Rønningsen et al. (1997), Lira et al. (1996), Pan et al. (1997) and the Coutinho model, among others.

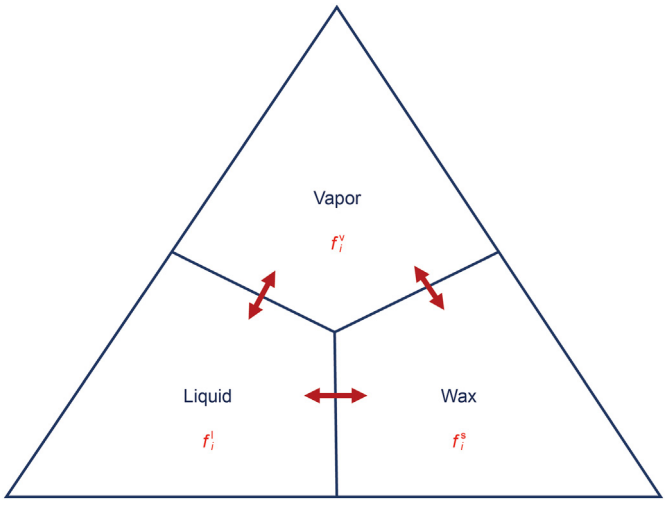

Fig. 5. Illustration of equilibrium state for a wax system (Leontaritis, 1996).

Accordingly, the vapor-liquid fugacities are calculated using the cubic equations of state (EOS) in the earlier models. For instance, in the Pedersen model, the Soave-Redlich-Kwong equation of state (SRK) (Eq. (2)) was used (Lin et al., 2006; Pedersen, 1995; Pedersen et al., 1984; Sandarusi et al., 1986; Soave, 1972), whereas the Lira et al. model uses the Peng Robinson equation of state (PR-EOS) shown in Eq. (3) (Lira et al., 1996; Peng and Robinson, 1976).

$$P = \frac{RT}{V-b} - \frac{\alpha(T)}{V(V+b)} \tag{2}$$

$$P = \frac{RT}{V-b} - \frac{\alpha(T)}{V(V+b)+b(V-b)} \tag{3}$$

The temperature-dependent term $\alpha(T)$ and volume-dependent term b of the mixture are obtained with mixing rules. Different mixing rules have been suggested over the years, and in the case of the Lira et al. model, the Chueh and Prausnitz (1967) rules were used.

While the liquid-gas phase fugacities can be determined using the equations of state, this is not the case with the solids. In solid-state, activity coefficient models are used.

In 1986, Won used a modified regular solution model to determine the activities of liquid-solid components that were calculated using solubility parameters (Eqs. (4) and (5)) and used the SRK-EOS for gas-liquid phases (Won, 1986).

$$\delta_i^{\mathrm{l}} = \sqrt{\frac{\Delta H_i^{\mathrm{vap}} - RT}{V_i^{\mathrm{l}}}} \tag{4}$$

$$\delta_i^{\mathrm{s}} = \sqrt{\frac{\Delta H_i^{\mathrm{vap}} - \Delta H_i^{\mathrm{f}} - RT}{V_i^{\mathrm{s}}}} \tag{5}$$

where δ_i^{l} and δ_i^{s} represent the solubility parameters, $\Delta H_i^{\mathrm{vap}}$, ΔH_i^{f} are vaporization and fusion enthalpies and V_i^{l}, V_i^{s} are volume fractions. Won proposed the use of correlations to determine the $\Delta H_i^{\mathrm{vap}}$, ΔH_i^{f}, V_i^{l}, and V_i^{s} parameters.

Initially, this model neglected the change in heat capacities of the phases and their overall impact on the fugacities of the solid/liquid pure components. It also did not account for pressure dependence as well as the gas phase.

Later, Hansen et al. conducted a research study on seventeen oil mixtures. They used the Flory-Huggins polymer-solution theory (Flory, 1953) to account for the non-idealities in the liquid phase while maintaining the activity of the solid phase to a constant of 1 (Hansen et al., 1988). It was observed that Won's 1986 wax model was not efficient in determining wax appearance temperature and amounts. Won revised his 1986 model to include the effect of heat capacities (ΔC_{P}), on the equilibrium constant and used a more rigorous regular solution model to determine the activity coefficients. Instead of using solubility parameters, fugacity and composition relations for every phase were introduced. It was assumed that the difference in partial volume was significantly small and that the heavy hydrocarbon components were in a pure solid phase (Won, 1989). Using the relationship between fugacities of a component in pure solid and pure liquid at a given pressure (P), together with the fugacity of the same component in the

homogeneous wax phase, Won developed an expression to determine the component's fugacity in the solid phase Eq. (6).

$$f_i^{os}(P) = f_i^{ol}(P)\exp\left[-\frac{\Delta H_i^f}{RT}\left(1-\frac{T}{T_i^f}\right)+\frac{\Delta C_{P_i}}{R}\left(1-\frac{T_i^f}{T}+In\frac{T_i^f}{T}\right)\right] \quad (6)$$

where f_i^{ol}, f_i^{os} are liquid and solid fugacities respectively; ΔH_i^f is the change in fusion enthalpy; ΔC_{P_i} is the change in heat capacities; T_i^f is fusion temperature and R is ideal gas constant. The determined activities were in the range of 0.7–1.0, but it was later found that the model was more limited to the liquid and solid phases, minimizing the contribution of the gas phase (Hansen et al., 1988; Pedersen, 1995; Pedersen et al., 1991). Later, it was also determined that there was no relation between the liquid and solid phase activities as earlier thought (Meray et al., 1993). In 1991, Pedersen et al. discovered that both the Hansen et al. and the Won models gave higher WAT and overestimated the amount of wax deposited. (Pedersen et al., 1991)

Consequently, the Pedersen model (Pedersen, 1995), later modified by Rønningsen et al. (1997), used the regular solution expression and incorporated modified fusion enthalpies for the pseudo components into the Won wax model. The model also used two adjustable parameters for change in heat capacity, and C_{7+} split pseudo components. These models provided better cloud point estimates and Pedersen suggested the use of higher fugacities for some pseudo components to avoid overestimation of wax amount (Pedersen, 1995). The model used the SRK equation of state for the vapor-liquid phases and the ideal solid solution theory for the wax/solid phase. It was proposed that only the C_{7+} components can form wax, and similarly, only a tiny fraction of these components contribute to wax formation. The mole fraction distribution of the C_{7+} wax forming components can be determined as per Eq. (7).

$$z_i^s = z_i^{tot}\left[1-(A+BM_i)\left(\frac{\rho_i-\rho_i^P}{\rho_i^P}\right)^C\right] \quad (7)$$

where z_i^{tot} is the total mole fraction for carbon fraction *i*. *A, B, C* are empirical constants and ρ_i^P is the density of normal paraffins with same mole weight as fraction, *i*.

Furthermore, the model was based on the assumption that influence due to change in heat capacities of the solid and liquid phases was minimal and could be neglected in the determination of fugacities of the components in the wax phase, as shown in Eq. (8) (Pedersen, 1995; Rønningsen et al., 1997).

$$f_l^s = x_i^s\varphi_i^{ol}(P)\exp\left[-\frac{\Delta H_i^f}{RT}\left(1-\frac{T}{T_i^f}\right)+\frac{\Delta V_i\left(P-P_{ref}\right)}{RT}\right] \quad (8)$$

The fugacity, f_i^{ol}, of pure component, *i*, in liquid was calculated using the SRK EOS and is equivalent to $x_i^s\varnothing_i^{ol}(P)$ term in the equation above. ΔV_i was presumed at 10% of the hydrocarbon molar volume in the liquid phase.

Lira et al. (1996) developed a multi-solid wax thermodynamic model based on thermal stability analysis and demonstrated the effect of heat capacity difference on equilibrium determination among others. They determined solidified phases (pseudo components) using the stability test criterion (Elliott and Lira, 1999) whilst using an equation of state (Peng-Robinson) and activity model for liquid-vapor and solid-liquid phases, respectively. According to the model results, it was shown that, on average, the precipitated wax was mainly composed of paraffins with carbon numbers greater than 25. As suggested in earlier models, the model required no adjusted parameters for mixtures.

Pan et al., in 1997 were able to distinctively divide each petroleum cut into cycloalkanes and the aromatics (Pan et al., 1997). They assigned properties to these cuts, including those with molecular weights greater than 300 using correlations by Lira et al. (1996) and Lee-Kesler (Lee and Kesler, 1975). Their work laid the foundation for more rigorous thermodynamic modeling.

Subsequently, the Coutinho model took the wax thermodynamic modeling a step further. The postulated model takes into account the impact of entropy due to differences in molecular size and volume effects (Coutinho, 1998; Coutinho and Daridon, 2001; Coutinho et al., 2006; Yang et al., 2016). This was made possible by modeling the liquid state non-idealities using the Flory free volume theory (Coutinho, 1998). The model as well provided flexibility and meticulous handling of the solid phase non-idealities whereby both the Wilson model and Universal Quasichemical (UNIQAC) activity coefficient models can be used (Do Carmo et al., 2018). In a 2006 research study, Coutinho et al. (2006) evaluated the results of this model on predicting wax amount whilst using both the activity models and concluded that the results were close to experimental data from the Differential scanning calorimetry and Microscopy (Fig. 6).

Based on experimental data and model results from Pan et al. (1997) study, Dalirsefat and Feyzi (2007) developed a model that only considered the $C_{15}+$ hydrocarbons as wax-forming molecules. Their model eliminated contribution from the lighter components. Likewise, the solution theory was used for the solid-liquid system and a modified Peng Robinson EOS for the liquid gas system. They correlated the heat capacity change (ΔC_{P_i}) using the Pedersen et al. correlations and melting points using the Lira et al. relations.

Over the years, the models have been upgraded to incorporate both the UNIQUAC and Functional Group activity coefficients models to handle non-idealities in the liquid phase. The models can be used to cater for possible secondary phase transitions during wax formation. This rigorous modeling has to some extent, provided quite accepted results. Noticeably, most models use the SRK or the PR cubic equations of state to handle non-idealities in a liquid-vapor system. Since its debut in 2001, the Perturbed-Chain Statistical Associating Fluid theory (PC-SAFT) equation of state (Gross and Sadowski, 2001, 2002) has been used to characterize fluid systems, including heavy hydrocarbon systems (Diamantonis et al., 2013; Gonzalez et al., 2005). Per the model results, PC-SAFT

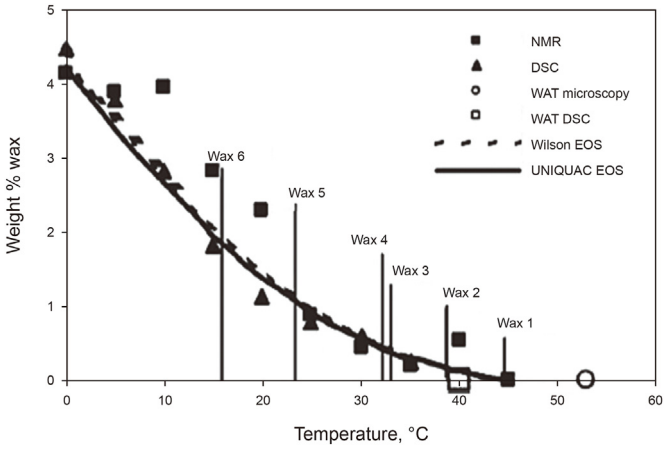

Fig. 6. Wax precipitation curves as determined using the UNIQUAC and Wilson activity models Adapted with permission from Coutinho et al. (2006). Copyright © 2006, American Chemical Society.

improved the understanding of wax precipitation in crude oil. An example is the works by Bagherinia et al. (2016), Meighani et al. (2018), and Shahsenov et al. (2021) in which the fluid system was handled using the PC-SAFT, whereas the solid-liquid non-idealities were handled using the UNIQUAC activity model.

In most wax thermodynamic modeling studies, it has been observed that the results are quite satisfactory in regards to their respective experiment data. This scenario leaves more to researchers to find the best way to meticulously model and handle the wax non-idealities in solution depending on a particular crude oil. Pauly et al. performed a comparative analysis of the Coutinho, Won, and the Pedersen model (Pauly et al., 1998). It is observed that the Coutinho model results fit well the experimental data hence suitable for wax determination compared to other models. Fig. 7.

In the past half-decade, researchers have made several modifications and innovations to the pre-existing thermodynamic models to improve WAT and Wax precipitation curve (WPC) predictions in recent years. Yang et al. (2016) proposed using Flory free-volume and regular solution models to account for enthalpy, entropy, and energy interactions in the Liquid phase while adopting the use of Wilson EOS and a modified regular solution model to cater for the solid phase. The models reflected improved prediction in WPC and WAT per the study's experimental results. In a study published in 2018, scientists Kazmierczak et al. conducted a comprehensive analysis of the thermophysical correlations used during modeling. It was found that the thermodynamic models strongly depend on the thermal physical properties of the n-paraffins (Kazmierczak et al., 2018). Thus, suggested two wax prediction approaches: the multi-solid phase model and the solid solution model. The assumptions made are that each solid phase in the multi-solid model consists of a pure component while only one solid is formed in the solid solution model.

Mansourpoor et al. (2019) suggested a multi-solid model for WAT prediction. In their model, PNA (naphthenic-aromatic) analysis and two correlations for the PNA species are introduced in the legacy models. Besides, in a closely related study, the researchers attempted to use artificial neural networks (ANN) and new empirical correlations to correct for inconsistencies in legacy models using pressure, molecular weight, and specific gravity as inputs for neural networks.

Bagherinia et al. (2019) proposed prediction based on using PC-SAFT in a multi-solid framework to improve wax prediction using their earlier model that was anchored on using the UNIQUAC activity model for solids and a PC-SAFT EOS for the solid-solution state. Per the research results, their modified model produced better accuracy than the earlier model.

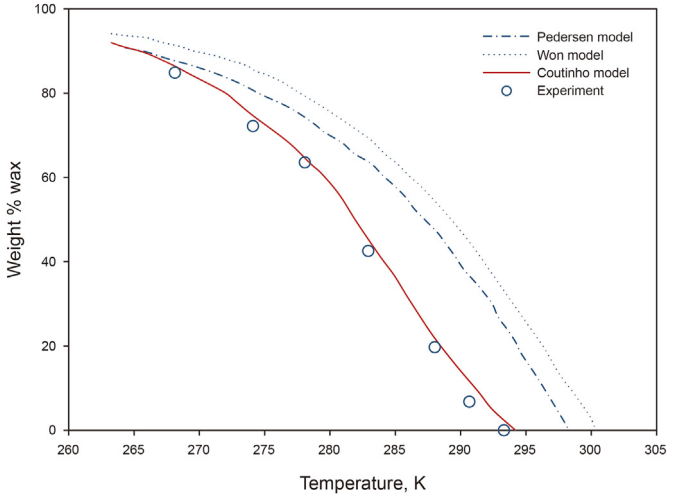

Fig. 7. Graph of wax precipitation curves determined using different models and compared to experimental data. Adapted with permission from Pauly et al. (1998). Copyright © 1998 Elsevier Science B.V. All rights reserved.

In research by Heidariyan et al. (2019), a modified predictive thermodynamic model is proposed that couples the multi-solid model with PC-SAFT and Peng Robison equations of state. The model accounts for pressure effects on the total system. At pressures above the bubble point, the solid-liquid equilibrium calculations are done, while at lower pressures, the ternary phase equilibria calculations are done to predict the WAT. Thus, the researchers could lower the discrepancies in estimations close to the bubble point conditions. Xue et al. (2019) postulated a general thermodynamic model that predicts wax and asphaltene precipitation, catering for up to four phases in the system. In the study, a simplified-PC-SAFT EOS (sPC-SAFT) is suggested for wax/asphaltenes mixtures, while the UNIQUAC model for non-idealities in the predominant wax phase. Besides, a modified correlation is used to predict the BIPs using measured binary solid solubilities for the $C_{12}+$ n-alkane mixtures.

Furthermore, Wang and Chen (2020) postulated an explicit co-crystal model predicting wax formation at low pressures. The model uses a simplified Flory-Huggins EOS to cater for non-idealities in the liquid phase. The study contemplates an explicit co-crystallization of n-paraffins dependent on the variations in carbon number for wax forming species. The co-crystallization process forms perfect multi-component molecular crystals with compatible structures and sizes hence the hypothesis that co-crystallization is ideal at a molecular level. However, it is noted that the model only inputs properties of pure components which may limit its broad application.

Asbaghi and Assareh (2021) suggested a thermodynamic model based on sequential equilibrium calculation steps using a multi-solid framework. Moreover, Asbaghi et al. (2021) proposed improving wax prediction using PC-SAFT by modifying the binary interaction parameters (BIPs) used for the non-wax forming species. In the model, PC-SAFT EOS is used for the liquid state. The BIPs and variations in heat capacities for the liquid-solid state are modified to minimize deviations caused by averaging hydrocarbons' properties.

Most recently, Sulaimon and Falade (2022) have proposed two new multi-component thermodynamic models: two-phase and three-phase models. The two-phase model uses a three-parameter gamma distribution function, while the three-phase model is based on the regular solution and the legacy equation of states. The alpha, beta, and eta parameters of the gamma function are used to classify hydrocarbon mixtures into waxy/asphaltenic oils, condensate/light oils, and biodegraded oils. Besides, they developed new correlations for the thermophysical properties characterizing the hydrocarbon species. According to the published data, while the models satisfactorily predict WAT for waxy/asphaltenic oils and condensate/light oils, they overestimated the point in biodegraded oils.

3.2. Deposition models

Wax deposition models, also known as kinetic models, have undergone various modifications to attain more accuracy. Modeling is mainly centered on the use of the depositional mechanisms, and in some models, parameters are fitted with experimental data. Generally, the amount of wax deposited in the pipe is a function of temperature and time (Alnaimat and Ziauddin, 2020; Singh et al., 2000). As the temperature decreases, the paraffin concentration in the solution state decreases and increases in the solid-state. Sarica and Panacharoensawad (2012) did extensive reporting on deposition in multi-phase flows models. In this section, a

discussion is presented on models that have been used to model depositions under all types of flow conditions (Single, binary, and multi-phase flows).

3.2.1. Single-phase flow

There are quite several single-phase flow models that various research teams have suggested. Similar to thermodynamic modeling, deposition rate modeling as well dates back to the 1980s'. Among the earliest models are the Burger et al. (1981), Hamouda and Ravneøy (1992), and Hsu et al. (1994) models in that order. In the Burger mathematical model, modeling was based on molecular diffusion and dispersion mechanisms. The model neglects the other mechanisms. The Hamouda model is an improvement of the Burger model that includes the aging and stripping mechanisms though it falls short of accounting for deposition in various regime flows.

In the Hsu et al. model, modeling included the molecular diffusion and dispersion effects to predict the deposition rate. Unlike earlier models, the researchers performed calculations at conditions similar to pipe flow velocity and flow regime. However, it is complicated because it is difficult to harmonize the flow regimes at these standards since they will vary with the dimensions of flow even when the velocities are matched.

3.2.1.1. Singh et al. model. In this model, it was recognized that aging and stripping have a significant impact on the wax deposition rate and could not be neglected in the modeling process. Accordingly, the conservation of mass is based on the assumption that the rate of change of wax in the deposit is equivalent to the radial convective flux of wax molecules with the exclusion of those in the oil. Singh et al. (2000) incorporated the diffusion effect into the gel. Thus, the deposit growth, J_g, was given as per Eq. (9) and later was also adopted by Hernandez et al. (2003).

$$Jg = Jc - Jd - Js \tag{9}$$

where, J_d, J_c and J_s refer to the mass flux diffused into the deposit (kg/m^2s), mass flux from bulk to surface (kg/m^2s), mass flux (kg/m^2s) sheared from the deposit respectively. These are correspondingly given as:

$$Jd = -De\frac{dCe}{dT}\frac{dT}{dr}\bigg|_{r=r_w} \tag{10}$$

$$Jc = K_m(C_{wb} - C_{wi}) \tag{11}$$

$$Jg = Jc[1 - \varphi(Fw)] - Js. \tag{12}$$

where D_e is effective diffusivity, k_m is the convective mass transfer coefficient (kg/m^2s), C_e is the equilibrium concentration at temperature, T, while C_{wb} is wax concentration in the fluid, and C_{wi} is the wax concentration at the fluid-deposit interface. F_w is wax fraction in the deposit.

3.2.1.2. Hernandez et al. model. The calculation for total wax accumulated in deposit was summarized in the expression:

Numerically this is expressed as per Eq. (13) (Hernandez et al., 2003).

$$\frac{d}{dt}\left[\pi\left(r_i^2 - r_w^2\right)L\rho\right] = \frac{2\pi r_w J_g}{F_w}L \tag{13}$$

where L is the length of pipe, r_i is the inner radius, r_w is radius with wax deposit, ρ is the fluid density, t is time and J_g is the net mass flux directed towards deposit growth (kg/m^2s). F_w is the fraction of wax in the deposit, while δ refers to the thickness of the wax deposit.

The convection mass transfer to the interface term, J_c, used is similar to those used in the earlier models following the Tulsa university model (Matzain, 1996). In both the Singh et al. (2000) and Hernandez et al. (2003) models, the impact due to solidification is catered for in the effective diffusivity (D_e), which in itself is a function of porosity for wax structure. In both studies the Cussler et al. (1988) expression for diffusivity in a porous flaky media was used, Eq. (14).

$$De = \frac{Dwo}{1 + \alpha^2 F_w^2/(1 - F_w)} \tag{14}$$

D_{wo} is the molecular diffusivity of wax in oil (m^2/s), α is aspect ratio of the wax crystals, F_w refers to the weight fraction of solid wax in the gel.

After simplification and numerically solving equations, Eq. (15) is obtained, and it represents the mass balance.

$$\frac{d\delta}{dt} = \frac{Jc[1 - \varphi(Fw)] - Js}{\rho Fw} \tag{15}$$

Finally, Hernandez et al. suggest an overall model for wax balance in the deposit in Eq. (16)

$$\frac{dFw}{dt} = \frac{[Jc\varphi(Fw)]2(r_i - \delta)}{\rho\delta(2r_i - \delta)} \tag{16}$$

3.2.1.3. Huang et al. model. The team observed that not all wax crystals would deposit on the pipe wall. Based on this assumption, together with Fick's diffusion law, they developed a less complex prediction model with relatively satisfactory results compared to its earlier peers. The numerical model is as per Eq. (17).

$$W = k\tau_w^m\frac{1}{\mu}\left(\frac{dC}{dT}\right)\left(\frac{dT}{dr}\right)^{n+1} \tag{17}$$

where τ_w is the shear stress (Pa), $\frac{dC}{dT}$, $\frac{dT}{dr}$ are changes in wax volume with respect to temperature and radial temperature change respectively, m, k, and n are constants obtained through experimentation.

3.2.2. Binary phase flow

Unlike single-phase models, mathematical modeling in the binary and multi-phase flow is complex. Still, in recent years, a few

$$\textit{Total accumulated Wax} = \textit{Mass diffusivity to deposit} - \textit{Oil diffusivity from deposit} + \textit{Wax to new deposit volume} - \textit{Net mass of sheared wax} + \textit{Net gain/loss of oil due to new deposit volume}$$

scholarly teams have made significant strides in this area, especially binary phase flow. This section reviews deposition rate modeling in the gas-oil and water-oil phase flows.

3.2.2.1. Gas-Oil phase flow. The majority of the research studies on this phase flow have concluded that gas in oil lowers the wax depositional rate (Zougari, 2010) yet is still affected by flow regimes. In vertical flow, the deposit is thicker in laminar when compared to transitional and turbulent flows (Matzain et al., 2001; Sarica and Panacharoensawad, 2012). In contrast, slug flow tends to deposit wax along the entire pipe section.

Numerical modeling for depositional rate in the gas-oil phase flow is entirely based on Fick's law of diffusion. Recent research works were conducted by Matzain et al., 2001, 2002 and Duan et al. (2017).

The Matzain et al. gas-oil depositional model considers both shearing and oil locked in the deposited matrix (Apte et al., 2001; Matzain et al., 2001, 2002). Based on these mechanisms, the model somewhat predicts wax deposition rate as per Eq. (18).

$$\frac{d\delta}{dt} = \frac{\prod_1}{1+\prod_2} D_{OW}\left(\frac{dC_W}{dT}\frac{dT}{dr}\right) \tag{18}$$

The derivatives $\frac{dC_W}{dT}$, $\frac{dT}{dr}$ represent changes in wax concentration with respect to radial temperature and temperature with respect to the internal radius of the pipe, respectively. The terms Π_1, Π_2 are empirical correlations for porosity and shear dispersion effects, respectively (Leporini et al., 2019; Wilke and Chang, 1955). The porosity correlation reflects the wax deposition caused by the oil displaced in the wax deposition layer, whereas Π_2 accounts for wax molecules removed from the deposited layer.

However, follow-up research studies have shown that the model requires improvement due to less accuracy in slug and stratified flow regimes (Apte et al., 2001; Matzain et al., 2001, 2002).

The Duan et al. (2017) model is a much more recent model that fairly predicts deposition in mostly stratified flows. The calculations are based on the assumption that the flow in the pipe is fully developed, and simplification of the mathematical expressions yields Eq. (19).

$$\frac{d\delta}{dt} = -\frac{\left(D_{OW}\frac{\partial C}{\partial r}\big|_{r_i} - D_e\frac{\partial C}{\partial r}\big|_{r_i^+}\right)}{\rho_{dep}F_W} \tag{19}$$

where $d\delta/dt$ is the rate of deposition, ρ_{dep} is deposit density (kg/m^3), r is the inner radius of pipe (m), D_{ow} and D_e are the wax diffusivities in oil and the effective diffusivity, respectively. F_w is the wax fraction in the deposit (wt %), and C is the wax concentration (kg/m^3).

3.2.2.2. Oil-water flows. In oil production, oil formation in water emulsions is almost unavoidable for various reasons like shear flows due to pumping actions. As earlier discussed, dispersed phases significantly impact the wax formation process (Bazooyar et al., 2020; Guo and Li, 2017). Depending on various factors like flow regimes, wetting characteristics, and the amount of the individual phases, this binary flow system contributes to wax depositions. In dynamic conditions, Zhang et al. (2010) observed that the deposition rate is unaffected by the volume of the individual phases. While in a study by Wang et al. (2018), it was discovered that in static conditions, the water content has an impact on the amount of heat dissipated from the system, which in turn affects the diffusion mechanism.

However, it is to be noted that perhaps this effect is correlated with the decrease in the temperature difference rather than the water content.

Wet surfaces significantly lower wax deposition on pipe walls (Couto et al., 2008), but the effect depends on the contact area in laminar and turbulent flow regimes. In laminar regimes, deposition occurs when the oil phase makes contact with the wall surface but in turbulent flow only when the phase is directly contacted (Couto et al., 2008). These effects are also related to the composition of the oil. They vary with different oils; thus, several research studies need to be conducted before a general conclusion can be made.

Numerical and mathematical models for this phase flow include but are not limited to Couto et al. (2008), Bruno et al. (2008), Zhou et al. (2016), and Zheng et al. (2017) models. These models are mainly improvements of earlier suggested single-phase models.

3.2.3. Multi-phase flow

The Couto et al. model is mainly suited for static conditions and utilizes the single-phase mathematical model parameters to predict wax deposition rate. It was designed based on the University of Tulsa single-phase model (Matzain, 1996). The physical properties and solubility of the system are expressed as functions of the water fraction. The physical properties include viscosity, heat capacity, density, and molecular weight, which are obtained using equations (20) through (23). Brinkman's correlation was used for the calculation of viscosity, whereas the thermal conductivities for deposition and emulsion were calculated using the Maxwell correlations, Eq. (24) (Bruno et al., 2008; Couto et al., 2008; Jaeger and Carslaw, 1959).

$$\mu_{sol} = \mu_{cont}(1-\varphi_{int})^{-2.5} \tag{20}$$

$$C_{pmix} = w_o C_{po} + w_w C_{pw} \tag{21}$$

$$\rho_{mix} = f_o\rho_o + f_w\rho_w \tag{22}$$

$$M_{mix} = x_o M_o + x_w M_w \tag{23}$$

where μ_{sol}, μ_{cont} represent viscosities of emulsion and the continuous phase while the Φ_{int} term is volume fraction for internal phase. C_{pmix}, C_{po}, and C_{pw} are respectively the mixture, oil, and water heat capacities. w_o, w_w are oil and water weight fractions in that order. ρ_{mix}, ρ_o and ρ_w are the mixture, oil, and water densities, whereas f_o, f_w are volume fractions for oil and water. The terms M_{mix}, M_o, M_w are molecular weights for the mixture, oil, and water, whereas x_o, x_w are molar fractions for water and oil, respectively.

$$K_{dep} = \frac{2K_w + K_{mix} + (K_w - K_{mix})F_w}{2K_w + K_{mix} - 2(K_w - K_{mix})F_w} \tag{24}$$

The K_{mix} is given by the following equation,

$$K_{mix} = K_o\left\{1 + \left(\frac{3F_c}{K_w + 2K_o/K_w - K_o} - F_c\right)\right\} \tag{25}$$

The terms K_{mix}, K_{dep}, K_o , K_w refer to the thermal conductivities (W/(mK)) measured in oil, water, water-oil mixture, and deposit phases, respectively. F_c represents the amount of water in the emulsion, whereas F_w is the fraction of water in the deposit.

The Bruno et al. (2008) model improves the Couto et al. (2008) model. The viscosity correlation in the Couto model is substituted with the Richardson correlation due to its high performance at high water cuts. The team developed a correlation for trapped water given in Eq. (26) and proposed using a modified equation (Eq. (27)) to determine the diffusion coefficient, given that diffusion is limited

at higher water cuts.

$$f_{w,dep} = 0.0283e^{2.4184 f_{w,bulk}} \tag{26}$$

$$D_{o/w} = D_{w/o}\left(1 - f_{w,bulk}\right) \tag{27}$$

where $f_{w,dep}$, $f_{w,bulk}$ are respectively fractions of water, wax deposit, and oil/water mixture. $D_{o/w}$ is the diffusion coefficient of the oil-in-water emulsion (m^2/s) and $D_{w/o}$ is water in oil diffusion coefficient (m^2/s).

Similar to most models, this model also fails to incorporate the effects of different flow regimes in predicting wax deposition.

Zhou et al. (2016) suggested a numerical model for calculating deposition rate suited for mainly laminar flows, Eq. (28). However, because this model is tailored for laminar flows, prediction in variant flow regimes is less accurate.

$$\frac{d\delta}{dt} = \frac{\rho_{oil}}{\rho_{dep}}\left\{\frac{D_{OW}\frac{dC_{wax}}{dT}\frac{dT}{dr}}{F'_w} + \frac{k(C - C_{int})}{F'_w(1 - \varphi_{wm})}\exp\left(\frac{T_{pp}}{T_{int}}\right)f\right\} \tag{28}$$

where ρ_{oil}, ρ_{dep} are oil and deposit densities (kg/m^3), D_{wo} is the molecular diffusivity in oil (m^2/s). C_{wax} and C_{int} refer to wax solubilities in bulk oil and oil at the deposition interface, T is the temperature (K), F'_w is the wax amount after dehydration (%), k is gelling adhesion coefficient (m/s), $\varnothing_{wm}$ refers to the mass water mass cut in the emulsion deposit (%), T_{pp} is pour point (°C), T_{int} is the temperature at the flow interface (°C), and f is shear stress.

In addition to the Matzain et al. model, other models are mostly incorporated into commercial simulation software (Leporini et al., 2019). The models relatively simulate wax deposition scenarios in pipelines to a reasonable degree. Notable ones include Rygg, Rydahl and Rønningsen model (RRR model) and Heat analogy.

The RRR model is one of the few multi-phase flow deposition models on the market. The model still maintains shearing as a significant contributor to the amount of wax deposited. It calculates accumulated wax using both molecular diffusion and shearing mechanisms as simplified in Eq. (29).

$$\dot{\delta} = \frac{\delta_{diff} + \delta_{shear}}{2\pi r_s L(1 - \varphi_{wax})} \tag{29}$$

where δ is the total rate of deposit accumulation. δ_{diff}, δ_{shear} are accumulation rates due to molecular diffusion and shearing mechanism, respectively. L is the length of the pipe/well, r_s is the starting internal pipe diameter, whereas $\varnothing_{wax}$ is the wax porosity within the range $0.6 \leq \varnothing_{wax} \leq 0.9$ (Edmonds et al., 2008).

While details and data published on the heat analogy model are scant, in a few articles, it was reported that the model considers the relationship between heat transfer and mass transfer to account for the amount of wax deposited in the pipe. These quantities are indirectly determined and correlated using the Nusselt and Sherwood numbers (Kumar and Mahulikar, 2017; Leporini et al., 2019; Mehrotra et al., 2020; Reay et al., 2013).

Leporini et al. (2019) performed a detailed evaluation of these models in a three-phase flow system. Their study compares field results to simulation results using commercial software like Leda-Flow, Schlumberger's OLGA, and KBC's FloWax, among others. Most recently, Shahdi and Panacharoensawad (2019) developed an open-source wax prediction software (SP-Wax) for predicting wax formation in crude oil. The software utilizes a solid-liquid equilibria approach based on the Coutinho et al. thermodynamic model to estimate WAT, deposit aging, and solid-phase composition.

4. Wax deposition experimentation

Depending on the experimental conditions, Wax deposition experimentation methods are categorized into dynamic and static. In Table 1, a summary of these methods is provided.

5. Wax prevention techniques

As the saying goes, “prevention is better than cure”; it is of great significance to prevent wax deposition than its removal. This is not only from an economic point of view but also for health, safety, and environmental considerations.

One of the recent innovations in remediating wax precipitation is the use of nanocomposite pourpoint depressants (NPPDs) (Wang et al., 2020; Yu et al., 2019). These depressants are reported to alter the crystallization morphology of wax crystals that causes a reduction in yield stress of wax deposits in pipes (Huang et al., 2019). Peng et al. (2021), Yu et al. (2019), and Huang et al. (2020) extensively reported that the efficacy of pourpoint depressants is significantly amplified when magnetic fields of optimum frequency and intensity are applied to deposit locations.

Sharma et al. (2022) conducted a research study in which graphene oxide nanocomposites and ionic liquids are postulated to depress the wax pourpoint. The study presents the use of Octyl 3-methylimidazolium chloride ionic liquid, which, per the study results, caused a 46% reduction in the pourpoint. On the other hand, the graphene nanocomposites caused a ~76% reduction when applied to the Indian waxy oil.

Nonetheless, engineers and researchers have suggested several methods to prevent wax deposition over the years. These techniques are categorized into mechanical, chemical, and biological. In Tables 2 and 3, mechanical and chemical methods are summarized.

5.1. Biological methods

This technique involves using bacteria and their metabolites to adsorb onto the pipe walls or on the sucker rods. The adsorption of microbial bacteria can form a protective film on the tube wall, which prevents the wax crystal from adsorbing on the tube wall. At the same time, the process of microbial metabolism can degrade the long-chain alkanes in the crude oil, thus reducing the viscosity and improving oil flow. Likewise, the metabolic processes may produce some surface-active substance that can be adsorbed on the pipe wall. These substances can create a reverse wetting effect that minimizes wall depositions.

6. Wax removal techniques

Timely and well-planned removal of wax deposits is necessary to maintain normal operations. Wax accumulations in the wells can cause a multitude of issues like breakage of rods due to overloading and sticking of maintenance tools inside the well, among others. In Table 4, the most recent reported wax removal techniques are summarized.

7. Prospective future research

The influence of flow regimes on wax deposition remains a prospective research area. Field studies show that deposition rate varies for different flow regimes (laminar, turbulent, etc.). Severe cases occur mainly for turbulent flows; hence, comprehensive studies of this phenomenon are needed to provide general trends and predictive models. Moreover, available models for wax deposition need updating to improve prediction. The main reason is that the current models focus on single and binary phase flows. Future

Table 1
Wax deposition experimental methods.

Name	Test conditions	Operation	Remarks	Reference
Cold finger or Cold Plate (Static and Dynamic)	• Laminar and Turbulent • Batch volumes are supported. • Cold plates can be curved or flat (~3 mm thick). • Cold fingers are up to 40 mm in diameter. • Magnetic stirring is supported	• A temperature-controlled rod or plate is immersed into the oil sample whose temperature keeps falling. The finger/Plate represents pipe wall conditions and can be held at environmental temperature. • The rod is removed and weighed to determine the wax deposit upon completion. • Under dynamic conditions, a rotary agitator is added to the device to evaluate the shearing effect.	• The method is cheap, requires less sample, is fast and convenient. • The dynamic device is more favorable since it mimics reality. • But it should be noted that the setup is far from a real pipeline setting	(Mahir et al., 2018; Morozov et al., 2016; Zougari, 2010)
Organic Solids deposition and Control System (OSDC) (Dynamic)	• Allows all flow regimes • Controlled shearing • Volume about 150 cm^3 • Temperature range from −20 to 200 °C • Pressure up to 105 MPa	• The device has a Coquette-Taylor flow similar to a cold finger but with improvements to simulate single and binary phase flows at high-pressure conditions. • It offers better hydrodynamics and the ability to include roughness effects.	• Allows phase flow simulation and high accuracy under high pressure and shearing conditions. • Cleaning can be such a tedious task.	Zougari et al. (2006)
Rotary device (Dynamic)	• Shearing ranges between 12 and 5000s^{-1} • Flow-through and batch volumes are supported • In case of flow-through; pipe dimeter is about 6 mm. • Heat transfer (19 −5800 W/m^2)	• Consists of both sample and wax cylinder. • The sample holder is rotated to mimic real flow, while the wax cylinder is positioned in the sample holder is adjusted to simulate shearing using a torque sensor	• While still not satisfactory to real situation standards and need for high sample volumes, the setup affords good insulation and temperature control • Sloughing is likely if wall stress exceeds deposit strength	(C. Li et al., 2014; Matlach and Newberry, 1983)
Flow loop (Dynamic)	• Volume depends mostly on loop pipe diameter. • Loop diameter ranges (6 −40 mm ID), lengths up to 40 m • Shearing ranges between 330 and 1330 s^{-1} • Laminar-turbulent flows depend on experiment design	• It consists of both cold and hot utilities. • The loop is an actual pipe of reasonable dimensions. Its wall temperature is set to the test environment, and deposit thickness is evaluated using differential pressure. • Recent advancements have included laser technology to evaluate the deposit thickness	• Widely preferred in wax deposition experimentation. • The setup is capable of simulating real flow conditions. • However, the method is cumbersome, costly, and sophisticated.	(Ehsani et al., 2019; Hoffmann et al., 2012; S. Li et al., 2014)

works would improve these models by incorporating three-phase flow data. Three-phase and multi-flow phases are more common than binary and single-phase flow in field production. Besides, except for molecular diffusion, others mechanisms for wax deposition are still debatable, and experimental verification is yet to be realized.

Computational fluid dynamics and molecular simulation studies are other areas that require further research. These would provide more understanding of molecular dynamics and microfluidics concerning wax deposition.

Currently, climate change is a major global concern, and finding green sustainable solutions is paramount. This predicament opens new doors to research and design for environmentally friendly wax mitigation techniques.

Lastly, wax analytical methods also need to be upgraded, especially for early detection of wax formation. Presently, there is no published research on artificial intelligence techniques in the early detection and mitigation of wax and other colloidal deposition problems. This field could be a great research opportunity, especially in High pressure/High-temperature wells.

8. Conclusion

This review discusses the chemical composition, thermodynamic and kinetic modeling, and inhibition and removal techniques for crude oil wax. Further research is needed for multi-phase flows such as gas-oil-water and gas-oil-water-hydrates, among others. Concisely, this article provides interested researchers with a concise catch-up on research progress in this field and provides a reference for future works.

Table 2
Summary of mechanical wax prevention techniques.

Method	Description	Remarks	Reference
Cold seeding	• Involves injecting "cold seeds" into the bulk oil to initiate wax deposition in oil. The seeds may be oil wax and polyethylene pellets. • The seeds essentially act as nucleation sites that maintain deposition within the bulk of the oil other than the pipe wall. Likewise, the pellets can act as crystal modifiers that prevent the wax crystals from aggregating. • If oil wax is used, a certain quantity of oil is separated from the main line and chilled at low temperatures to deposit wax. Together with wax is re-injected into the main line as cold seeds.	1. Reported to have been used in Canada and in the United States. 2. Applicable on surface pipelines. 3. Less information is available for injection profiles and optimization of this technique.	(Al-Yaari, 2011; Nenniger, 1991, 2001)
High Pressure-Shear Heat Exchangers	• Heat exchangers (heat sinks) are used to deposit wax crystals that are quickly sheared using high-pressure pumps hence decelerating deposition. • Pressure surges together with pigs can be used. The surges create a sonic effect that dislodges deposits in the pipe.	1. This mechanism would suggest a turbulent flow thus can exacerbate deposition. 2. Can be used both in walls, sea and land surface lines.	(Al-Yaari, 2011; Fung et al., 2003)
Flash cooling	• Gas is injected into the oil via a valve to cause a throttle expansion, creating a Joule-Thomson effect. • This lowers the temperature in the mid-stream flow reversing the temperature gradient. Instead of deposition, a slurry flow is formed.	1. Proper insulation is needed which increases costs. 2. Effectiveness remains to be evaluated.	(Elliott and Lira, 1999; Knowles, 1987; Reif, 2009)
Fluid (oil/solvent) injection	• Similar to flash cooling, cold oil or solvent is injected in this case.	1. Applicable in wells, sea, and surface environments. 2. Unsustainable for very long lines.	(Al-Yaari, 2011; Hutton and Kruka, 2001; Nenniger, 2001)
Thermal Heating and Insulation	• Electric heaters (bottom-hole heaters, cables) heat the pipes above Wax appearance temperature. • Low thermal conductive materials like polyurethane provide insulation, thus minimizing heat loss and energy consumption.	1. Highly effective and widely used. 2. Burning out of cables may occur. 3. Applicable in all environments. Cheap in wells but costly for long lines	(Bosch et al., 1992; Danilović et al., 2010; Kovrigin and Kukharchuk, 2016)
Sonic, Magnetic, and Electric field	• Sonication slows deposition and dislodges deposits. • Strong electric/magnetic fields across the pipe induce polarization of tiny wax crystals averting heavy crystal formation.	1. Applicable in reservoirs, wells, and pipelines. 2. May disrupt life in aquatic habitants	(Hamida and Babadagli, 2007; Hou et al., 2015; Mullakaev et al., 2015; Roberts et al., 2000; Tao and Tang, 2014; Tao and Xu, 2006)

Table 3
Summary of chemical wax prevention techniques.

Method	Description	Remarks	Reference
Chemical Coatings	• Chemicals are cast inside pipe walls to minimize adhesion and to alter wettability properties like oleophobicity and hydrophobicity. • Used chemicals are resistant to corrosion and abrasion. • Glass-reinforced epoxy resins and plastic coating are widely reported. • Likewise, metallic coatings like carbon hybrid diamonds and polymers like oxazolane-based polymers and fluoro-siloxanes can be cast inside pipes.	1. The technique minimizes deposition and promotes slurry flow. 2. Some coatings may act as insulators. 3. Applicable in all environments. 4. Coated pipes are pretty costly.	(Dvornic et al., 2004; Li et al., 2003; Paso et al., 2009; Z. Wang et al., 2013)
Wax inhibitors/Crystal modifiers	• Inhibitors can be comb polymers, ethylene copolymers, and polymers with long alkyl groups. The polymers adsorb onto the walls better than wax molecules and affect the fluidity of the oil. • Crystal modifiers bond with wax molecules and avert their aggregation. Mostly used are polymeric forms of ethylene, acrylates, fatty esters, vinyl pyridines, and copolymers of ethylene with vinyl acetate. • Mixtures of ethylene-vinyl acetate and α-olefinic maleic anhydrides are also common.	1. Efficacy depends on the frequency of side chains and similarity in chain lengths. 2. Polymers soluble at $<15^0$C are effective in oils with 20%wt wax. 3. Tailor-made chemicals are frequently needed which are time-consuming and costly.	(Binks et al., 2015; Chen et al., 2010; Hennessy et al., 2004; Pedersen and Rønningsen, 2003)
Ethylene polymers and copolymers	• Mainly include ethylene polymer or small alkene copolymers; ethylene polymer and acrylonitrile copolymer; and ethylene polymer with vinyl acetate. Ethylene with vinyl acetate (EVA) is the most known and used among ethylene copolymers. • Act as nucleation sites and lower the crystallinity of the wax molecules while promoting solubility.	1. Functionality depends on the amount of vinyl acetate (VA). 2. Hydrolyzed EVA of 20-30% VA composition is most effective for wax inhibition. 3. Polymers are safe to use and environmentally friendly	(Machado and Lucas, 2002; Machado et al., 2001; Marie et al., 2005)
Comb polymers	• Have a "comb" like design and a polyvinyl backbone anchoring numerous long chain side groups. • This structure minimizes wax aggregation through steric hindrance and bonding with wax molecules. • Monomers are mainly maleic anhydride and (meth) acrylate ester polymers or a mixture of both. • Other varieties used as flow improvers include: Stearyl acrylate and ally polyglycol copolymers blended with poly-isobutylene and alkyl-phenol formaldehyde resins.	1. Better pour point depression than ethylene polymers. 2. For high WAT, they need blending with other chemicals, which increases costs. 3. Safe to use and environmentally friendly.	(Bello et al., 2006; Brunelli and Fouquay, 2001; Duffy and Rodger, 2002; Kelland, 2014; Wei, 2015)

Table 4
Summary of wax removal techniques used in the oil industry.

Method	Description	Remarks	Reference
Mechanical removal	• Oldest and most widely used methods to remove wax depositions inside wells. • Involves cutting the tubing or scrapping the deposit from the tubing with "pigs." • The scrappers or cutters are mounted on sucker rods or deployed using a wireline. These tools adjust to the width of the tube to maintain contact. • Different pigs have been invented over the years, like bypass pigs	1. For hard deposits, chemicals are good supplements. 2. Quite inexpensive. 3. Can increase pipe roughness that accelerates deposition. 4. Scrapping and cutting can deposit solids in the well that require fishing.	(Al-Yaari, 2011; Fung et al., 2006)
Thermal	• Supply heat energy that melts wax deposits; reduces viscosity; and improves flowability. Heat sources are heat carriers, electrical heaters, and thermochemical methods. • The heat carriers are hot oil, hot water circulation systems, steam injection, and heaters in the form of spiral cables on the exterior of the pipes or installed at the bottom of wells. • Recent advancements include thermochemical techniques. Inductive heating through exothermic chemical reactions heats the blocked sections of the pipe. Reactions include light metals (Magnesium, Aluminum, etc.) with HCl, $NaNO_2$, or $NaNO_3$ reacting with NH_4Cl and other active metals.	1. Suitable in all environments 2. Hot water circulation is preferred to hot oiling. Water is cheap, has fewer contaminants, has high specific heat capacity, and is readily available. 3. Hot oiling can lead to the devaluation of oil. 4. Control over exothermic reactions downhole is complex and corrosive reactions are possible. 5. It can be costly for long flows and in sea environments.	(Al-Yaari, 2011; Nguyen et al., 2001; Sarmento et al., 2004; Thota and Onyeanuna, 2016; Tiwari et al., 2014; Zhang et al., 2007; Zyrin and Vasiliev, 2016)
Chemical	• Mainly include dispersants, solvents, and emulsifiers. • Wax dispersants/detergents keep crystals spread in oil, averting interaction and aggregation. Can also alter surface properties like wettability. An example is 2-amino-ethyl-2-alkyl-imidazoline. • Solvents are mainly water-based, organic, and emulsifiers. Organ solvents like xylene and light crude distillates are used, among others • Emulsifiers combine both effects of organic and water-based solvents to dislodge wax deposits. • Emulsification leads to high shearing and low interfacial tension, lowering the deposition rate.	1. Can lower pour point by 300C. 2. Some field applications require mixing surfactants with dispersants for maximum efficiency. 3. Blends of dispersants and polymeric inhibitors are more effective. 4. Solvent efficiency depends on chemistry and temperature. Some are fire risks like CS_2. 5. Chemical removal is costly.	(Ahn et al., 2005; Groffe et al., 2001; Kelland, 2014; Manka et al., 1999; San-Miguel and Rodger, 2000; Wang et al., 2003)
Biological	• Involves the use of bacteria to degrade wax deposits in flow lines. • Bacteria of genera Pseudomonas and Bacillus show great potential. They digest long-chain hydrocarbons that form wax. • Some bacteria function like bio-surfactants that can reverse wettability on pipe surfaces. This reduces adhesion, promotes emulsion, reduces depositions • It is possible to increase production while at the same time remediating wax issues.	1. Reduction in Carbon footprint hence environmentally friendly. 2. Special conditions are required for the continuous growth of the bacteria. 3. Still no evidence that oil equality is unaffected.	(He et al., 2003; Rana et al., 2010; Santamaria and George, 1991; Xiao et al., 2012)

Declaration of competing interest

The authors declare no competing financial interest.

Acknowledgments

The authors would like to acknowledge contributions from colleagues and support from Sinopec Company limited (Project P19018-2) and the National Natural Science Foundation of China (52174047).

Appendix A. Supplementary data

Supplementary data to this article can be found online at https://doi.org/10.1016/j.petsci.2022.08.008.

References

Ahn, S., Wang, K., Shuler, P., Creek, J., Tang, Y., 2005. Paraffin crystal and deposition control by emulsification. In: Paper Presented at the SPE International Symposium on Oilfield Chemistry. https://doi.org/10.2118/93357-MS.

Al-Yaari, M., 2011. Paraffin wax deposition: mitigation and removal techniques. In: Paper Presented at the SPE Saudi Arabia Section Young Professionals Technical Symposium. https://doi.org/10.2118/155412-MS.

Alnaimat, F., Ziauddin, M., 2020. Wax deposition and prediction in petroleum pipelines. J. Petrol. Sci. Eng. 184, 106385. https://doi.org/10.1016/j.petrol.2019.106385.

Apte, M.S., Matzain, A., Zhang, H.Q., Volk, M., Brill, J.P., Creek, J.L., 2001. Investigation of paraffin deposition during multiphase flow in pipelines and wellbores-part 2: modeling. J. Energy Resour. Technol. 123 (2), 150–157. https://doi.org/10.1115/1.1484392.

Asbaghi, E.V., Assareh, M., 2021. Application of a sequential multi-solid-liquid equilibrium approach using PC-SAFT for accurate estimation of wax formation. Fuel 284, 119010. https://doi.org/10.1016/j.fuel.2020.119010.

Asbaghi, E.V., Assareh, M., Nazari, F., 2021. An effective procedure for wax formation modeling using multi-solid approach and PC-SAFT EOS for petroleum fluids with PNA characterization. J. Petrol. Sci. Eng. 207, 109103. https://doi.org/10.1016/j.petrol.2021.109103.

Bagherinia, R., Assareh, M., Feyzi, F., 2016. An improved thermodynamic model for Wax precipitation using a UNIQUAC+ PC-SAFT approach. Fluid Phase Equil. 425, 21–30. https://doi.org/10.1016/j.fluid.2016.05.008.

Bagherinia, R., Assareh, M., Feyzi, F., 2019. Thermodynamic modelling of wax precipitation using PC-SAFT in a multi-solid framework. Int. J. Oil Gas Coal Technol. 21 (2), 229–249. https://doi.org/10.1504/ijogct.2019.10021154.

Bai, Y., Bai, Q., 2018. Subsea Engineering Handbook. Gulf Professional Publishing.

Batsberg, P.W., Hansen, B.A., Larsen, E., Nielsen, A.B., Roenningsen, H.P., 1991. Wax precipitation from North Sea crude oils. 2. Solid-phase content as function of temperature determined by pulsed NMR. Energy Fuels 5 (6), 908–913. https://doi.org/10.1021/ef00030a020.

Bazooyar, B., Shaahmadi, F., Jomekian, A., Darabkhani, H.G., 2020. Modelling of wax deposition by perturbed hard sphere chain equation of state. J. Petrol. Sci. Eng. 185, 106657. https://doi.org/10.1016/j.petrol.2019.106657.

Bello, O., Fasesan, S., Teodoriu, C., Reinicke, K., 2006. An evaluation of the performance of selected wax inhibitors on paraffin deposition of Nigerian crude oils. Petrol. Sci. Technol. 24 (2), 195–206. https://doi.org/10.1081/lft-200044504.
Benamara, C., Nait Amar, M., Gharbi, K., Hamada, B., 2019. Modeling wax disappearance temperature using advanced intelligent frameworks. Energy Fuels 33 (11), 10959–10968. https://doi.org/10.1021/acs.energyfuels.9b03296.
Binks, B.P., Fletcher, P.D., Roberts, N.A., Dunkerley, J., Greenfield, H., Mastrangelo, A., Trickett, K., 2015. How polymer additives reduce the pour point of hydrocarbon solvents containing wax crystals. Phys. Chem. Chem. Phys. 17 (6), 4107–4117. https://doi.org/10.1039/C404329D.
Bird, R.B., 2002. Transport phenomena. Appl. Mech. Rev. 55 (1), R1–R4.
Bosch, F.G., Schmitt, K.J., Eastlund, B.J., 1992. Evaluation of downhole electric impedance heating systems for paraffin control in oil wells. IEEE Trans. Ind. Appl. 28 (1), 190–195. https://doi.org/10.1109/28.120230.
Brunelli, J.F., Fouquay, S., 2001. Acrylic copolymers as additives for inhibiting paraffin deposition in crude oils, and compositions containing same. In: Google Patents.
Bruno, A., Sarica, C., Chen, H., Volk, M., 2008. Paraffin deposition during the flow of water-in-oil and oil-in-water dispersions in pipes. In: Paper Presented at the SPE Annual Technical Conference and Exhibition. https://doi.org/10.2118/114747-MS.
Burger, E., Perkins, T., Striegler, J., 1981. Studies of wax deposition in the trans Alaska pipeline. J. Petrol. Technol. 33 (6). https://doi.org/10.2118/8788-PA, 1,075-071,086.
Chen, W., Zhao, Z., Yin, C., 2010. The interaction of waxes with pour point depressants. Fuel 89 (5), 1127–1132. https://doi.org/10.1016/j.fuel.2009.12.005.
Chueh, P., Prausnitz, J., 1967. Vapor-liquid equilibria at high pressures. Vapor-phase fugacity coefficients in nonpolar and quantum-gas mixtures. Ind. Eng. Chem. Fundam. 6 (4), 492–498. https://doi.org/10.1021/i160024a003.
Coutinho, J.A., 1998. Predictive UNIQUAC: a new model for the description of multiphase solid– liquid equilibria in complex hydrocarbon mixtures. Ind. Eng. Chem. Res. 37 (12), 4870–4875. https://doi.org/10.1021/ie980340h.
Coutinho, J.A., Daridon, J.L., 2001. Low-pressure modeling of wax formation in crude oils. Energy Fuels 15 (6), 1454–1460. https://doi.org/10.1021/ef010072r.
Coutinho, J.A., Edmonds, B., Moorwood, T., Szczepanski, R., Zhang, X., 2006. Reliable wax predictions for flow assurance. In: European Petroleum Conference. OnePetro. https://doi.org/10.2118/78324-MS.
Couto, G.H., Chen, H., Delle-case, E., Sarica, C., Volk, M., 2008. An investigation of two-phase oil/water paraffin deposition. SPE Prod. Oper. 23 (1), 49–55. https://doi.org/10.2118/114735-PA.
Cussler, E., Hughes, S.E., Ward III, W.J., Aris, R., 1988. Barrier membranes. J. Membr. Sci. 38 (2), 161–174. https://doi.org/10.1016/S0376-7388(00)80877-7.
Dalirsefat, R., Feyzi, F., 2007. A thermodynamic model for wax deposition phenomena. Fuel 86 (10–11), 1402–1408. https://doi.org/10.1016/j.fuel.2006.11.034.
Danilović, D.S., Karović-Maričić, V.D., Čokorilo, V.B., 2010. Solving paraffin deposition problem in tubing by heating cable application. Therm. Sci. 14 (1), 247–253. https://doi.org/10.2298/tsci1001247d.
Del Carmen Garcia, M., 2001. Paraffin deposition in oil production. In: Paper Presented at the SPE International Symposium on Oilfield Chemistry. https://doi.org/10.2118/64992-MS.
Diamantonis, N.I., Boulougouris, G.C., Mansoor, E., Tsangaris, D.M., Economou, I.G., 2013. Evaluation of cubic, SAFT, and PC-SAFT equations of state for the vapor–liquid equilibrium modeling of CO_2 mixtures with other gases. Ind. Eng. Chem. Res. 52 (10), 3933–3942. https://doi.org/10.1021/ie303248q.
Ding, J., Zhang, J., Li, H., Zhang, F., Yang, X., 2006. Flow behavior of Daqing waxy crude oil under simulated pipelining conditions. Energy Fuels 20 (6), 2531–2536. https://doi.org/10.1021/ef060153t.
Do Carmo, R.P., Da Silva, V.M., Fleming, F.P., Daridon, J.L., Pauly, J., Tavares, F.W., 2018. Paraffin solubility curves of diesel fuels from thermodynamic model adjusted through experimental DSC thermograms. Fuel 230, 266–273. https://doi.org/10.1016/j.fuel.2018.05.063.
Duan, J., Liu, H., Jiang, J., Xue, S., Wu, J., Gong, J., 2017. Numerical prediction of wax deposition in oil–gas stratified pipe flow. Int. J. Heat Mass Tran. 105, 279–289. https://doi.org/10.1016/j.ijheatmasstransfer.2016.09.082.
Duffy, D., Rodger, P., 2002. Modeling the activity of wax inhibitors: a case study of poly (octadecyl acrylate). J. Phys. Chem. B 106 (43), 11210–11217. https://doi.org/10.1021/jp026501j.
Dvornic, P.R., Hartmann-Thompson, C., Keinath, S.E., Hill, E.J., 2004. Organic–inorganic polyamidoamine (PAMAM) dendrimer– polyhedral oligosilsesquioxane (POSS) nanohybrids. Macromolecules 37 (20), 7818–7831. https://doi.org/10.1021/ma030542b.
Edmonds, B., Moorwood, T., Szczepanski, R., Zhang, X., 2008. Simulating wax deposition in pipelines for flow assurance. Energy Fuels 22 (2), 729–741. https://doi.org/10.1021/ef700434h.
Ehsani, S., Haj-Shafiei, S., Mehrotra, A.K., 2019. Deposition from waxy mixtures in a flow-loop apparatus under turbulent conditions: investigating the effect of suspended wax crystals in cold flow regime. Can. J. Chem. Eng. 97 (10), 2740–2751. https://doi.org/10.1002/cjce.23570.
Elliott, J.R., Lira, C.T., 1999. Introductory Chemical Engineering Thermodynamics, vol. 184. Prentice Hall PTR Upper, Saddle River, NJ.
Flory, P.J., 1953. Principles of Polymer Chemistry. Cornell University Press.
Fung, G., Backhaus, W., McDaniel, S., Erdogmus, M., 2006. To pig or not to pig: the marlin experience with stuck pig. In: Paper Presented at the Offshore Technology Conference. https://doi.org/10.4043/18387-MS.
Fung, G.S., Amin, R.M., Kalpakci, B., Fleyfel, F., O'sullivan, J.F., 2003. Method for reducing solids buildup in hydrocarbon streams produced from wells. In: Google Patents.
Gonzalez, D.L., Ting, P.D., Hirasaki, G.J., Chapman, W.G., 2005. Prediction of asphaltene instability under gas injection with the PC-SAFT equation of state. Energy Fuels 19 (4), 1230–1234. https://doi.org/10.1021/ef049782y.
Groffe, D., Groffe, P., Takhar, S., Andersen, S.I., Stenby, E.H., Lindeloff, N., Lundgren, M., 2001. A wax inhibition solution to problematic fields: a chemical remediation process. Petrol. Sci. Technol. 19 (1–2), 205–217. https://doi.org/10.1081/LFT-100001235.
Gross, J., Sadowski, G., 2001. Perturbed-chain SAFT: an equation of state based on a perturbation theory for chain molecules. Ind. Eng. Chem. Res. 40 (4), 1244–1260. https://doi.org/10.1021/ie0003887.
Gross, J., Sadowski, G., 2002. Application of the perturbed-chain SAFT equation of state to associating systems. Ind. Eng. Chem. Res. 41 (22), 5510–5515. https://doi.org/10.1021/ie010954d.
Guo, L., Li, W., 2017. The research status on wax deposition of waxy crude oil and its emulsions. Oil Gas Storage Transp. 36 (11), 1227–1236. https://doi.org/10.6047/j.issn.1000-8241.2017.11.001.
Haj-Shafiei, S., Workman, B., Trifkovic, M., Mehrotra, A.K., 2019. In-situ monitoring of paraffin wax crystal formation and growth. Cryst. Growth Des. 19 (5), 2830–2837. https://doi.org/10.1021/acs.cgd.9b00052.
Hamida, T., Babadagli, T., 2007. Analysis of capillary interaction and oil recovery under ultrasonic waves. Transport Porous Media 70 (2), 231–255. https://doi.org/10.1007/s11242-006-9097-9.
Hamouda, A., Ravneøy, J., 1992. Prediction of wax deposition in pipelines and field experience on the influence of wax on drag-reducer performance. In: Paper Presented at the Offshore Technology Conference. https://doi.org/10.4043/7060-MS.
Hansen, J.H., Fredenslund, A., Pedersen, K.S., Rønningsen, H.P., 1988. A thermodynamic model for predicting wax formation in crude oils. AIChE J. 34 (12), 1937–1942. https://doi.org/10.1002/aic.690341202.
He, Z., Mei, B., Wang, W., Sheng, J., Zhu, S., Wang, L., Yen, T., 2003. A pilot test using microbial paraffin-removal technology in Liaohe oilfield. Petrol. Sci. Technol. 21 (1–2), 201–210. https://doi.org/10.1081/LFT-120016942.
Heidariyan, H., Ehsani, M., Behbahani, T.J., Mohammadi, M., 2019. Experimental investigation and thermodynamic modeling of wax precipitation in crude oil using the multi-solid model and PC-SAFT EOS. Energy Fuels 33 (10), 9466–9479. https://doi.org/10.1021/acs.energyfuels.9b01445.
Hennessy, A., Neville, A., Roberts, K.J., 2004. In-situ SAXS/WAXS and turbidity studies of the structure and composition of multihomologous n-alkane waxes crystallized in the absence and presence of flow improving additive species. Cryst. Growth Des. 4 (5), 1069–1078. https://doi.org/10.1021/cg0341050.
Hernandez, O., Hensley, H., Sarica, C., Brill, J., Volk, M., Delle-Case, E., 2003. Improvements in single-phase paraffin deposition modeling. In: Paper Presented at the SPE Annual Technical Conference and Exhibition. https://doi.org/10.2118/84502-PA.
Hoffmann, R., Amundsen, L., Huang, Z., Zheng, S., Fogler, H.S., 2012. Wax deposition in stratified oil/water flow. Energy Fuels 26 (6), 3416–3423. https://doi.org/10.1021/ef2018989.
Hou, Y., Zhou, R., Long, X., Liu, P., Fu, Y., 2015. The design and simulation of new downhole vibration device about acoustic oil recovery technology. Petroleum 1 (3), 257–263. https://doi.org/10.1016/j.petlm.2015.09.001.
Hsu, J., Santamaria, M., Brubaker, J., 1994. Wax deposition of waxy live crudes under turbulent flow conditions. In: Paper Presented at the SPE Annual Technical Conference and Exhibition. https://doi.org/10.2118/28480-MS.
Huang, H.R., Wang, W., Peng, Z.H., Li, K., Ding, Y.F., Yu, W.J., Gan, D.Y., Xue, Y.H., Gong, J., 2020. Synergistic effect of magnetic field and nanocomposite pour point depressant on the yield stress of waxy model oil. Petrol. Sci. 17 (3), 838–848. https://doi.org/10.1007/s12182-019-00418-9.
Huang, H.R., Wang, W., Peng, Z.H., Li, K., Gan, D.Y., Zhang, S., Ding, Y.F., Wu, H.H., Gong, J., 2019. The effect of cooling processes on the yield stress of waxy model oil with nanocomposite pour point depressant. J. Petrol. Sci. Eng. 175, 828–837. https://doi.org/10.1016/j.petrol.2018.12.084.
Huang, Z., Lee, H.S., Senra, M., Fogler, H.S., 2011a. A fundamental model of wax deposition in subsea oil pipelines. AIChE J. 57 (11), 2955–2964. https://doi.org/10.1002/aic.15750.
Huang, Z., Lu, Y., Hoffmann, R., Amundsen, L., Fogler, H.S., 2011b. The effect of operating temperatures on wax deposition. Energy Fuels 25 (11), 5180–5188. https://doi.org/10.1021/ef201048w.
Hutton, G., Kruka, V., 2001. Existing Cold Flow Projects. DeepStar Report.
Jaeger, J.C., Carslaw, H.S., 1959. Conduction of Heat in Solids, second ed. Clarendon: Oxford University Press.
Kazmierczak, P.R., Paredes, M.L., Lima, E.R., Coutinho, J., 2018. A comparative analysis of thermophysical properties correlations for n-paraffins to be used in wax precipitation modeling. Fluid Phase Equil. 472, 172–184. https://doi.org/10.1016/j.fluid.2018.05.012.
Kelland, M.A., 2014. Production Chemicals for the Oil and Gas Industry. CRC press.
Knowles Jr., W.T., 1987. Choke cooling waxy oil. In: Google Patents.
Kovrigin, L., Kukharchuk, I., 2016. Automatic control system for removal of paraffin deposits in oil well in permafrost region by thermal method. Chem. Eng. Res. Des. 115, 116–121. https://doi.org/10.1016/j.cherd.2016.09.028.
Kumar, R., Mahulikar, S.P., 2017. Numerical re-examination of Chilton–Colburn analogy for variable thermophysical fluid properties. J. Heat Tran. 139 (7). https://doi.org/10.1115/1.4035855.
Lashkarbolooki, M., Esmaeilzadeh, F., Mowla, D., 2011. Mitigation of wax deposition

by wax-crystal modifier for Kermanshah crude oil. J. Dispersion Sci. Technol. 32 (7), 975–985. https://doi.org/10.1080/01932691.2010.488514.
Lashkarbolooki, M., Seyfaee, A., Esmaeilzadeh, F., Mowla, D., 2010. Experimental investigation of wax deposition in Kermanshah crude oil through a monitored flow loop apparatus. Energy Fuels 24 (2), 1234–1241. https://doi.org/10.1021/ef9010687.
Lee, B.I., Kesler, M.G., 1975. A generalized thermodynamic correlation based on three-parameter corresponding states. AIChE J. 21 (3), 510–527. https://doi.org/10.1002/aic.690210313.
Lee, D.G., Lim, J.S., Kim, Y.J., Woo, N.S., Han, S.M., Ha, J., 2020. Monitoring and detection of paraffin wax deposition process based on ultrasonic analysis. J. Nanosci. Nanotechnol. 20 (1), 168–176. https://doi.org/10.1166/jnn.2020.17282.
Leontaritis, K.J., 1996. The asphaltene and wax deposition envelopes. Fuel Sci. Technol. Int. 14 (1–2), 13–39. https://doi.org/10.1080/08843759608947560.
Leporini, M., Terenzi, A., Marchetti, B., Giacchetta, G., Corvaro, F., 2019. Experiences in numerical simulation of wax deposition in oil and multiphase pipelines: theory versus reality. J. Petrol. Sci. Eng. 174, 997–1008. https://doi.org/10.1016/j.petrol.2018.11.087.
Li, C., Bai, F., Wang, Y., 2014. Influence of crude oil composition on wax deposition on tubing walls. CIE J. 65 (11), 4571–4578. https://doi.org/10.3969/j.issn.0438-1157.2014.11.051.
Li, M., Zhai, J., Liu, H., Song, Y., Jiang, L., Zhu, D., 2003. Electrochemical deposition of conductive superhydrophobic zinc oxide thin films. J. Phys. Chem. B 107 (37), 9954–9957. https://doi.org/10.1021/jp035562u.
Li, S., Huang, Q., Wang, W., Wang, C., Ding, Z., 2014. Experimental investigation of wax deposition at different deposit locations through a detachable flow loop apparatus. In: Paper Presented at the International Pipeline Conference. https://doi.org/10.1115/IPC2014-33007.
Lin, H., Duan, Y.Y., Zhang, T., Huang, Z.M., 2006. Volumetric property improvement for the Soave– Redlich–Kwong equation of state. Ind. Eng. Chem. Res. 45 (5), 1829–1839. https://doi.org/10.1021/ie051058v.
Lira, G.C., Firoozabadi, A., Prausnitz, J.M., 1996. Thermodynamics of wax precipitation in petroleum mixtures. AIChE J. 42 (1), 239–248. https://doi.org/10.1002/aic.690420120.
Machado, A.L., Lucas, E.F., 2002. Influence of ethylene-co-vinyl acetate copolymers on the flow properties of wax synthetic systems. J. Appl. Polym. Sci. 85 (6), 1337–1348. https://doi.org/10.1002/app.10761.
Machado, A.L., Lucas, E.F., González, G., 2001. Poly (ethylene-co-vinyl acetate)(EVA) as wax inhibitor of a Brazilian crude oil: oil viscosity, pour point and phase behavior of organic solutions. J. Petrol. Sci. Eng. 32 (2–4), 159–165. https://doi.org/10.1016/S0920-4105(01)00158-9.
Mahir, L.H.A., Vilas, B.F.C., Ketjuntiwa, T., Fogler, H.S., Larson, R.G., 2018. Mechanism of wax deposition on cold surfaces: gelation and deposit aging. Energy Fuels 33 (5), 3776–3786. https://doi.org/10.1021/acs.energyfuels.8b03139.
Manka, J.S., Magyar, J.S., Smith, R.P., 1999. A novel method to winterize traditional pour point depressants. In: Paper Presented at the SPE Annual Technical Conference and Exhibition. https://doi.org/10.2118/56571-MS.
Mansourpoor, M., Azin, R., Osfouri, S., Izadpanah, A., 2019a. Experimental measurement and modeling study for estimation of wax disappearance temperature. J. Dispersion Sci. Technol. 40 (2), 161–170. https://doi.org/10.1080/01932691.2018.14616-35.
Mansourpoor, M., Azin, R., Osfouri, S., Izadpanah, A.A., 2019b. Study of wax disappearance temperature using multi-solid thermodynamic model. J. Pet. Explor. Prod. Technol. 9 (1), 437–448. https://doi.org/10.1080/01932691.2018.1461635.
Marie, E., Chevalier, Y., Eydoux, F., Germanaud, L., Flores, P., 2005. Control of n-alkanes crystallization by ethylene–vinyl acetate copolymers. J. Colloid Interface Sci. 290 (2), 406–418. https://doi.org/10.1016/j.jcis.2005.04.054.
Matlach, W., Newberry, M., 1983. Paraffin deposition and rheological evaluation of high wax content Altamont Crude Oils. In: Paper Presented at the SPE Rocky Mountain Regional Meeting. https://doi.org/10.2118/11851-MS.
Matzain, A., 1996. Single Phase Liquid Paraffin Deposition Modeling. University of Tulsa.
Matzain, A., Apte, M.S., Zhang, H.Q., Volk, M., Brill, J.P., Creek, J., 2002. Investigation of paraffin deposition during multiphase flow in pipelines and wellbores—part 1: experiments. J. Energy Resour. Technol. 124 (3), 180–186. https://doi.org/10.1115/1.1369359.
Matzain, A., Apte, M.S., Zhang, H.Q., Volk, M., Redus, C.L., Brill, J.P., Creek, J.L., 2001. Multiphase flow wax deposition modeling. In: Paper Presented at the Engineering Technology Conference on Energy. https://doi.org/10.1115/ETCE2001-17114.
Mehrotra, A.K., Ehsani, S., Haj-Shafiei, S., Kasumu, A.S., 2020. A review of heat-transfer mechanism for solid deposition from “waxy” or paraffinic mixtures. Can. J. Chem. Eng. 98 (12), 2463–2488. https://doi.org/10.1002/cjce.23829.
Meighani, H.M., Ghotbi, C., Behbahani, T.J., Sharifi, K., 2018. A new investigation of wax precipitation in Iranian crude oils: experimental method based on FTIR spectroscopy and theoretical predictions using PC-SAFT model. J. Mol. Liq. 249, 970–979. https://doi.org/10.1016/j.molliq.2017.11.110.
Meray, V.R., Volle, J.L., Schranz, C., Le Marechal, P., Behar, E., 1993. Influence of light ends on the onset crystallization temperature of waxy crudes within the frame of multiphase transport. In: Paper Presented at the SPE Annual Technical Conference and Exhibition. https://doi.org/10.2118/26549-MS.
Morozov, E.V., Falaleev, O.V., Martyanov, O.N., 2016. New insight into the wax precipitation process: in situ NMR imaging study in a cold finger cell. Energy Fuels 30 (11), 9003–9013. https://doi.org/10.1021/acs.energyfuels.6b01535.
Mullakaev, M., Abramov, V., Abramova, A., 2015. Development of ultrasonic equipment and technology for well stimulation and enhanced oil recovery. J. Petrol. Sci. Eng. 125, 201–208.
Nenniger, J., 1991. Process for Inhibiting Formation of Wax Deposits. CA Patent, 1289497.
Nenniger, J., 2001. Cold Seeding Lab Experiments. DeepStar Report. 4202-b4202.
Nguyen, D.A., Fogler, H.S., Chavadej, S., 2001. Fused chemical reactions. 2. Encapsulation: application to remediation of paraffin plugged pipelines. Ind. Eng. Chem. Res. 40 (23), 5058–5065. https://doi.org/10.1021/ie0009886.
Niesen, V., 2002. The Real Cost of Subsea Pigging. EP Magazine, p. 97.
Pan, H., Firoozabadi, A., Fotland, P., 1997. Pressure and composition effect on wax precipitation: experimental data and model results. SPE Prod. Facil. 12, 250–258. https://doi.org/10.2118/36740-PA, 04.
Paso, K., Kompalla, T., Aske, N., Rønningsen, H.P., Øye, G., Sjöblom, J., 2009. Novel surfaces with applicability for preventing wax deposition: a review. J. Dispersion Sci. Technol. 30 (6), 757–781. https://doi.org/10.1080/01932690802643220.
Pauly, J., Dauphin, C., Daridon, J., 1998. Liquid–solid equilibria in a decane+ multi-paraffins system. Fluid Phase Equil. 149 (1–2), 191–207. https://doi.org/10.1016/S0378-3812(98)00366-5.
Pedersen, K.S., 1995. Prediction of cloud point temperatures and amount of wax precipitation. SPE Prod. Facil. 10, 46–49. https://doi.org/10.2118/27629-PA, 01.
Pedersen, K.S., Rønningsen, H.P., 2003. Influence of wax inhibitors on wax appearance temperature, pour point, and viscosity of waxy crude oils. Energy Fuels 17 (2), 321–328. https://doi.org/10.1021/ef020142.
Pedersen, K.S., Skovborg, P., Roenningsen, H.P., 1991. Wax precipitation from North Sea crude oils. 4. Thermodynamic modeling. Energy Fuels 5 (6), 924–932. https://doi.org/10.1021/ef00030a022.
Pedersen, K.S., Thomassen, P., Fredenslund, A., 1984. Thermodynamics of petroleum mixtures containing heavy hydrocarbons. 1. Phase envelope calculations by use of the Soave-Redlich-Kwong equation of state. Ind. Eng. Chem. Process Des. Dev. 23 (1), 163–170. https://doi.org/10.1021/i200024a027.
Peng, D.Y., Robinson, D.B., 1976. A new two-constant equation of state. Ind. Eng. Chem. Fundam. 15 (1), 59–64. https://doi.org/10.1021/i160057a011.
Peng, Z., Yu, W., Yan, T., Huang, H., Gan, D., Wang, W., Gong, J., 2021. The synergic effect of a linear nanocomposite pour point depressant and magnetic field on the modification of highly waxy crude oil. J. Eng. Thermophys. 42 (3), 657–662.
Philp, R.P., Bishop, A., Del Rio, J.C., Allen, J., 1995. Characterization of high molecular weight hydrocarbons (> C_{40}) in oils and reservoir rocks. Spec. Publ. Geol. Soc. Lond. 86 (1), 71–85. https://doi.org/10.1144/GSL.SP.1995.086.01.06.
Quan, Q., Ran, W., Wang, S., Wang, Y., Li, R., Gong, J., 2019. Prediction the variation range of wax deposition with temperature of crude oil in a flow loop. Petrol. Sci. Technol. 37 (15), 1739–1746. https://doi.org/10.1080/10916466.2018.1511580.
Quan, Q., Wang, S., Sun, N., Wang, Y., Li, R., Gong, J., 2020. Experimental study on wax deposition of gas-liquid under intermittent flow. Petrol. Sci. Technol. 38 (4), 331–337. https://doi.org/10.1080/10916466.2019.1705854.
Rana, D.P., Bateja, S., Biswas, S.K., Kumar, A., Misra, T.R., Lal, B., 2010. Novel microbial process for mitigating wax deposition in down hole tubular and surface flow lines. In: Paper Presented at the SPE Oil and Gas India Conference and Exhibition. https://doi.org/10.2118/129002-MS.
Reay, D., Ramshaw, C., Harvey, A., 2013. Process Intensification: Engineering for Efficiency, Sustainability and Flexibility. Butterworth-Heinemann.
Reif, F., 2009. Fundamentals of Statistical and Thermal Physics. Waveland Press.
Roberts, P.M., Adinathan, V., Sharma, M.M., 2000. Ultrasonic removal of organic deposits and polymer induced formation damage. SPE Drill. Complet. 15 (1), 19–24. https://doi.org/10.2118/62046-PA.
Rønningsen, H., Sømme, B., Pedersen, K., 1997. An improved thermodynamic model for wax precipitation: experimental foundation and application. In: Paper Presented at the BHR Group Conference Series Publication. Retrived from: https://www.tib.eu/en/search/id/BLCP:CN020452302/An-improved-thermodynamic-model-for-wax-precipitation.
Rønningsen, H.P., 2012. Production of waxy oils on the Norwegian continental shelf: experiences, challenges, and practices. Energy Fuels 26 (7), 4124–4136. https://doi.org/10.1021/ef300288g.
Saffman, P., 1965. The lift on a small sphere in a slow shear flow. J. Fluid Mech. 22 (2), 385–400. https://doi.org/10.1017/S0022112065000824.
San-Miguel, M., Rodger, P., 2000. The effect of corrosion inhibitor films on deposition of wax to metal oxide surfaces. J. Mol. Struct.: THEOCHEM 506 (1–3), 263–272. https://doi.org/10.1016/S0166-1280(00)00418-8.
Sandarusi, J.A., Kidnay, A.J., Yesavage, V.F., 1986. Compilation of parameters for a polar fluid Soave-Redlich-Kwong equation of state. Ind. Eng. Chem. Process Des. Dev. 25 (4), 957–963. https://doi.org/10.1021/i200035a020.
Santamaria, M., George, R., 1991. Controlling paraffin-deposition-related problems by the use of bacteria treatments. In: Paper Presented at the SPE Annual Technical Conference and Exhibition. https://doi.org/10.2118/22851-MS.
Sarica, C., Panacharoensawad, E., 2012. Review of paraffin deposition research under multiphase flow conditions. Energy Fuels 26 (7), 3968–3978. https://doi.org/10.1021/ef300164q.
Sarmento, R., Ribbe, G., Azevedo, L., 2004. Wax blockage removal by inductive heating of subsea pipelines. Heat Tran. Eng. 25 (7), 2–12. https://doi.org/10.1080/01457630490495797.
Semenov, A.A., 2012. Wax deposition forecast. SPE Prod. Oper. 27 (4), 371–375. https://doi.org/10.2118/149793-PA.
Shahdi, A., Panacharoensawad, E., 2019. SP-Wax: solid–liquid equilibrium thermodynamic modeling software for paraffinic systems. SoftwareX 9, 145–153.

https://doi.org/10.1016/j.softx.2019.01.015.
Shahsenov, I., Baghishov, I., Allahverdiyev, P., Azizov, E., 2021. Wax precipitation modelling using perturbed chain statistical associating fluid theory (PC-SAFT). Fluid Phase Equil. 531, 112911. https://doi.org/10.1016/j.fluid.2020.112911.
Sharma, R., Deka, B., Mahto, V., Barifcani, A., Vuthaluru, H., 2022. Experimental investigation into the development and evaluation of ionic liquid and its graphene oxide nanocomposite as novel pour point depressants for waxy crude oil. J. Petrol. Sci. Eng. 208, 109691. https://doi.org/10.1016/j.petrol.2021.109691.
Singh, P., Venkatesan, R., Fogler, H.S., Nagarajan, N., 2000. Formation and aging of incipient thin film wax-oil gels. AlChE J. 46 (5), 1059–1074. https://doi.org/10.1002/aic.690460517.
Smith, J., Ness, V.H., Abbott, M., 1996. Introduction to Chemical Engineering Thermodynamics. McGraw Hill Chemical Engineering Series, p. 632.
Soave, G., 1972. Equilibrium constants from a modified Redlich-Kwong equation of state. Chem. Eng. Sci. 27 (6), 1197–1203. https://doi.org/10.1016/0009-2509(72)80096-4.
Sulaimon, A.A., Falade, G.K., 2022. New two-phase and three-phase thermodynamic models for predicting wax precipitation in hydrocarbon mixtures. J. Petrol. Sci. Eng. 208, 109707. https://doi.org/10.1016/j.petrol.2021.109707.
Suppiah, S., Ahmad, A., Alderson, C.J., Akbarzadeh, K., Gao, J., Shorthouse, J.M., Khan, I.A., Forde, C., Jamaluddin, A.K., 2010. Waxy crude production management in a deepwater subsea environment. In: Paper Presented at the SPE Annual Technical Conference and Exhibition. https://doi.org/10.2118/132615-PA.
Taheri-Shakib, J., Zojaji, I., Saadati, N., Kazemzadeh, E., Esfandiarian, A., Rajabi-Kochi, M., 2020. Investigating molecular interaction between wax and asphaltene: accounting for wax appearance temperature and crystallization. J. Petrol. Sci. Eng. 191, 107278. https://doi.org/10.1016/j.petrol.2020.107278.
Tao, R., Tang, H., 2014. Reducing viscosity of paraffin base crude oil with electric field for oil production and transportation. Fuel 118, 69–72. https://doi.org/10.1016/j.fuel.2013.10.056.
Tao, R., Xu, X., 2006. Reducing the viscosity of crude oil by pulsed electric or magnetic field. Energy Fuels 20 (5), 2046–2051. https://doi.org/10.1021/ef060072x.
Thota, S.T., Onyeanuna, C.C., 2016. Mitigation of wax in oil pipelines. Int. J. Eng. Res. Rev. 4 (4), 39–47. Retrived from online: https://www.researchpublish.com/papers/mitigation-of-wax-in-oil-pipelines.
Tiwari, S., Verma, S.K., Karthik, R., Singh, A.K., Kumar, S., Singh, M.K., Kothiyal, M.D., 2014. In-situ heat generation for near wellbore asphaltene and wax remediation. In: Paper Presented at International Petroleum Technology Conference. https://doi.org/10.2523/IPTC-17681-MS.
Wang, C., Zhang, M., Wang, W., Ma, Q., Zhang, S., Huang, H., Peng, Z.H., Yao, H.Y., Li, Q.P., Ding, Y., Gong, J., 2020. Experimental study of the effects of a nanocomposite pour point depressant on wax deposition. Energy Fuels 34 (10), 12239–12246. https://doi.org/10.1021/acs.energyfuels.0c02001.
Wang, K.S., Wu, C.H., Creek, J.L., Shuler, P.J., Tang, Y., 2003. Evaluation of effects of selected wax inhibitors on wax appearance and disappearance temperatures. Petrol. Sci. Technol. 21 (3–4), 359–368. https://doi.org/10.1081/LFT-120018525.
Wang, M., Chen, C.C., 2020. Predicting wax appearance temperature and precipitation profile of normal alkane systems: an explicit co-crystal model. Fluid Phase Equil. 509, 112466. https://doi.org/10.1016/j.fluid.2020.112466.
Wang, P., Wang, W., Gong, J., Zhou, Y., Yang, W., 2013. Effects of the dispersed phase on oil/water wax deposition. J. Energy Resour. Technol. 135 (4). https://doi.org/10.1115/1.4023932.
Wang, W., Huang, Q., Zheng, H., Li, S., Long, Z., Wang, Q., 2018. Investigation of wax deposition and effective diffusion coefficient in water-in-oil emulsion system. J. Therm. Anal. Calorim. 134 (2), 1031–1043. https://doi.org/10.1007/s10973-018-7385-6.
Wang, Z., Zhu, L., Liu, H., Li, W., 2013. A conversion coating on carbon steel with good anti-wax performance in crude oil. J. Petrol. Sci. Eng. 112, 266–272. https://doi.org/10.1016/j.petrol.2013.11.013.
Wei, B., 2015. Recent advances on mitigating wax problem using polymeric wax crystal modifier. J. Pet. Explor. Prod. Technol. 5 (4), 391–401. https://doi.org/10.1007/s13202-014-0146-6.
Wilke, C., Chang, P., 1955. Correlation of diffusion coefficients in dilute solutions. AIChE J. 1 (2), 264–270. https://doi.org/10.1002/aic.690010222.
Won, K., 1986. Thermodynamics for solid solution-liquid-vapor equilibria: wax phase formation from heavy hydrocarbon mixtures. Fluid Phase Equil. 30, 265–279. https://doi.org/10.1016/0378-3812(86)80061-9.
Won, K., 1989. Thermodynamic calculation of cloud point temperatures and wax phase compositions of refined hydrocarbon mixtures. Fluid Phase Equil. 53, 377–396. https://doi.org/10.1016/0378-3812(89)80104-9.
Xiao, M., Li, W.H., Lu, M., Zhang, Z.Z., Luo, Y.J., Qiao, W., Sun, S.S., Zhong, W., Zhang, M., 2012. Effect of microbial treatment on the prevention and removal of paraffin deposits on stainless steel surfaces. Bioresour. Technol. 124, 227–232. https://doi.org/10.1016/j.biortech.2012.07.063.
Xie, Y., Chen, D., Mai, F., 2018. Economic pigging cycles for low-throughput pipelines. Adv. Mech. Eng. 10 (11). https://doi.org/10.1177/1687814018811198, 1687814018811198.
Xiong, Q.Y., Kiyingi, W., Pan, J.J., Xiong, R., Deng, W., Zhang, S.L., Guo, J.X., Yang, Y., 2020a. Analysis of Xinjiang asphaltenes using high precision spectroscopy. RSC Adv. 10 (65), 39425–39433. https://doi.org/10.1039/D0RA07278H.
Xiong, R.Y., Guo, J.X., Kiyingi, W., Feng, H.S., Sun, T., Yang, X., Li, Q., 2020b. Method for judging the stability of asphaltenes in crude oil. ACS Omega 5 (34), 21420–21427. https://doi.org/10.1021/acsomega.0c01779.
Xue, J., Li, C., He, Q., 2019. Modeling of wax and asphaltene precipitation in crude oils using four-phase equilibrium. Fluid Phase Equil. 497, 122–132. https://doi.org/10.1016/j.fluid.2019.06.011.
Yang, J., Wang, W., Huang, H., Shi, G., Shi, B., Cheng, B., Gong, J., 2016. Prediction of solid-liquid equilibrium in paraffinic systems with new solid solution model. Fluid Phase Equil. 427, 504–512. https://doi.org/10.1016/j.fluid.2016.07.030.
Yu, H., Sun, Z., Jing, G., Zhen, Z., Liu, Y., Guo, K., 2019. Effect of a magnetic nanocomposite pour point depressant on the structural properties of daqing waxy crude oil. Energy Fuels 33 (JUL), 6069–6075. https://doi.org/10.1021/acs.energyfuels.9b00689.
Zhang, Y., Gong, J., Ren, Y., Wang, P., 2010. Effect of emulsion characteristics on wax deposition from water-in-waxy crude oil emulsions under static cooling conditions. Energy Fuels 24 (2), 1146–1155. https://doi.org/10.1021/ef901065c.
Zhang, Y., Qi, S., Shen, J., Li, X., Song, F., 2007. Rapid wax plugging removal using active metal alloy. Gasf. Surf. Eng. 6–7. https://doi.org/10.3969/j.issn.1-0066896.2007.08.003, 08.
Zheng, S., Fogler, H.S., Haji-Akbari, A., 2017. A fundamental wax deposition model for water-in-oil dispersed flows in subsea pipelines. AIChE J. 63 (9), 4201–4213. https://doi.org/10.1002/aic.15750.
Zhou, G., Xie, Z.W., Xu, X.H., Li, Q., 2020. A new model of overall heat transfer coefficient of hot wax oil pipeline based on dimensionless experimental analysis. Case Stud. Therm. Eng. 20, 100647. https://doi.org/10.1016/j.csite.2020.100647.
Zhou, Y., Gong, J., Wang, P., 2016. Modeling of wax deposition for water-in-oil dispersed flow. Asia Pac. J. Chem. Eng. 11 (1), 108–117. https://doi.org/10.1002/apj.1948.
Zougari, M., Jacobs, S., Ratulowski, J., Hammami, A., Broze, G., Flannery, M., Stankiewicz, A., Karan, K., 2006. Novel organic solids deposition and control device for live-oils: design and applications. Energy Fuels 20 (4), 1656–1663. https://doi.org/10.1021/ef050417w.
Zougari, M.I., 2010. Shear driven crude oil wax deposition evaluation. J. Petrol. Sci. Eng. 70 (1–2), 28–34. https://doi.org/10.1016/j.petrol.2009.01.011.
Zyrin, V.O., Vasiliev, B.U., 2016. Electrothermal complex with downhole electrical heating generators for enhanced heavy oil recovery. Int. J. Appl. Eng. Res. 11 (3), 1859–1866. Retrived from online: https://www.researchgate.net/publication/303699144_Electrothermal_complex_with_downhole_electrical_heating_generators_for_enhanced_heavy_oil_recovery.